ASIPP

Tungsten Atomic Data Needs in ASIPP and Relevant Activities

ZHANG Ling [1*], MORITA Shigeru [2,1], MITNIK Darío [3,1], DING Xiaobin [4],
YAO Ke [5], YANG Yang [5], XIAO Jun [5], LIU Haiqing [1]

[1] *Institute of plasma physics, Chinese Academy of Sciences, Hefei 230031, China*
[2] *National Institute for Fusion Science, Toki 509-5292, Gifu, Japan*
[3] *Universidad de Buenos Aires, Argentina*
[4] *Northwest Normal University, Lanzhou 730070, China*
[5] *Institute of Modern Physics, Fudan University, Shanghai 200433, China*

Acknowledgements: This work was supported by the National Magnetic Confinement Fusion Energy R&D Program of China (Grant Nos. 2022YFE03180400, 2022YFE03020004), National Natural Science Foundation of China (Grant No. 12322512), and Chinese Academy of Sciences President's International Fellowship Initiative (PIFI) (Grant Nos. 2024PVA0074, 2025PVA0060).

*Email: zhangling@ipp.ac.cn 29 August 2024

Outline

ASIPP

- Tungsten and High-Z impurity source in EAST
- Impurity-related spectroscopic diagnostics in EAST
- Tungsten data needs and other important issues
- Relevant Activities
- Summary

Outline

ASIPP

- Tungsten and High-Z impurity source in EAST
- Impurity-related spectroscopic diagnostics in EAST
- Tungsten data needs and other important issues
- Relevant Activities
- Summary

Upgrade of EAST divertors & first wall

Dr. ZI Pengfei

ASIPP

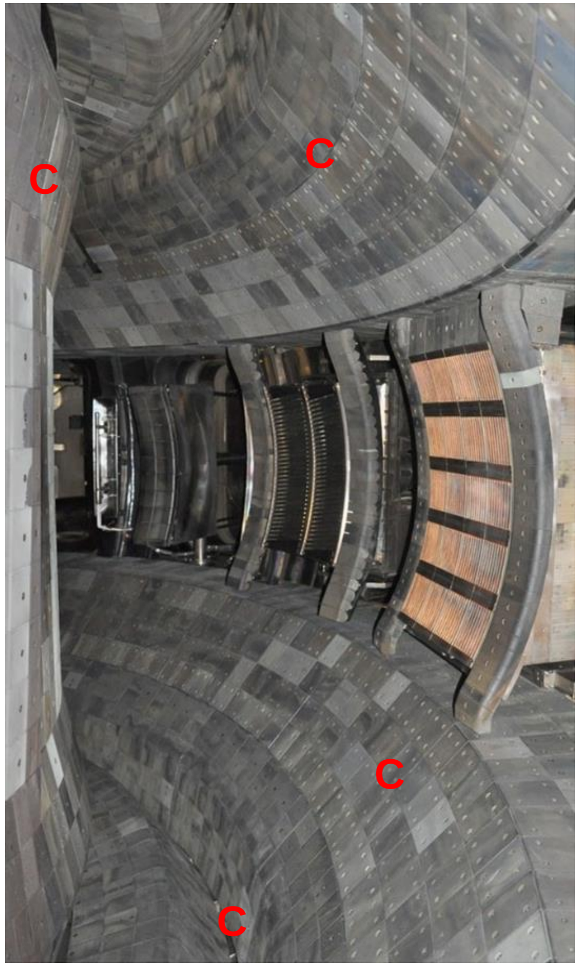

Carbon PFC (2008)
Max. 2 MW/m^2

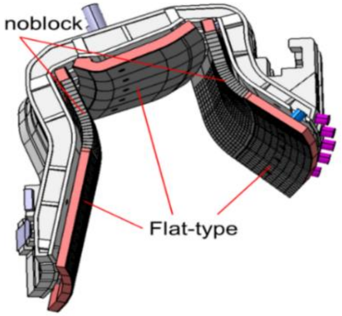

UPPER DIVERTOR (2012)

First W/Cu Divertor (Monoblock)

High / Low field side first wall (2010)

TZM (Titanium-Zirconium-Molybdenum) alloy

LOWER DIVERTOR 2021

W/Cu Divertor

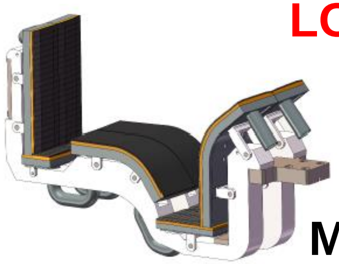

Monoblock

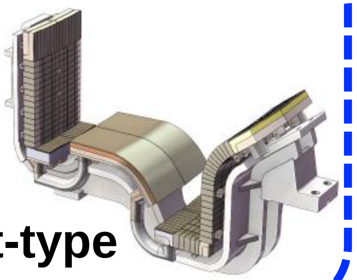

Flat-type

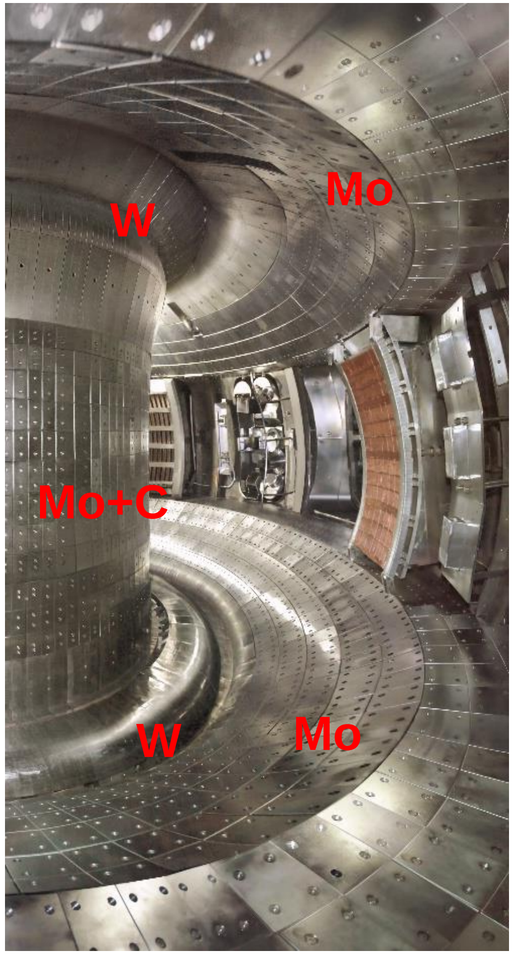

Metal PFC (2024)
Max. 10 MW/m^2

EAST major Limiter and antenna guard limiter

ASIPP

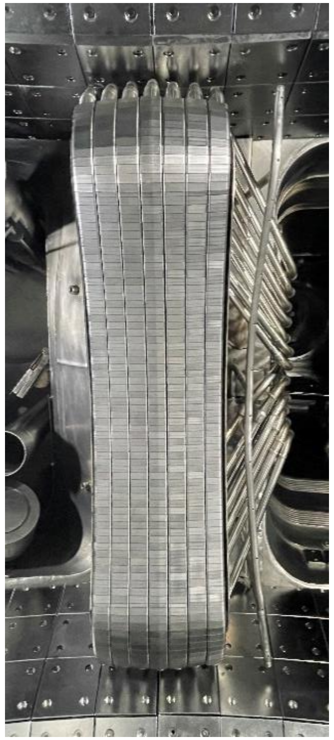

2023/11-present
7 Monoblock
HIP **W/Cu**
L=1, R=2.35, r=0.75 m

Guard limiter for LHW antenna

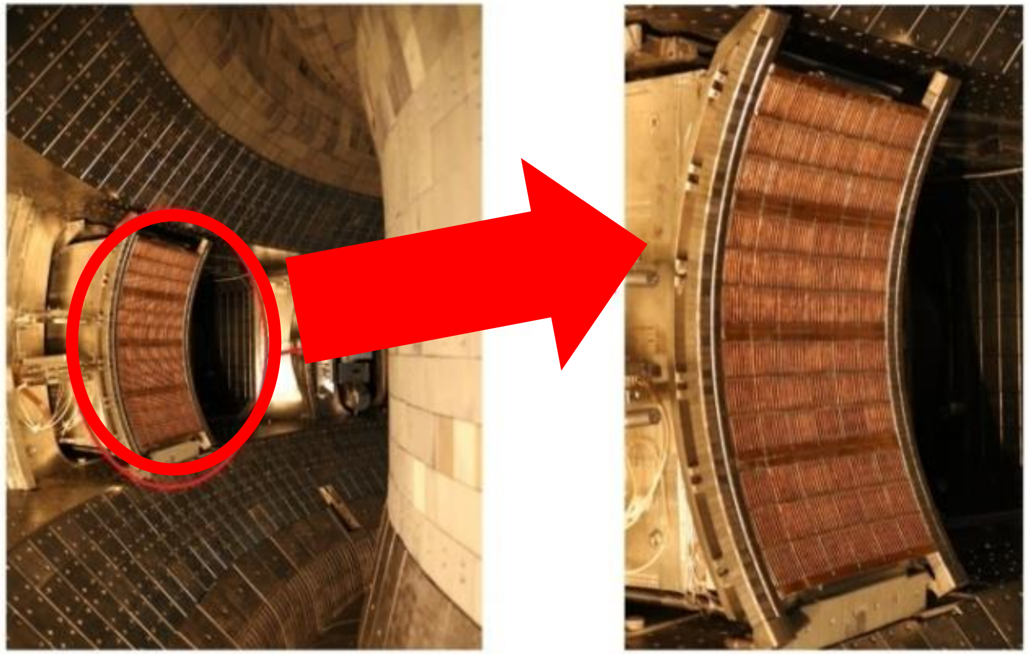

- **LHW / ICRF antenna: Cu / Fe**
- **Guard limiters: C → W (since 2018)**

Major limiter in EAST is located between port G and H

Dr. ZI Pengfei

Tungsten and high-Z impurity

ASIPP

High-Z impurity induced by heating system

RF Heating

[ICRF and LHW] Interaction with antenna and guard limiter: when the RF wave does not couple effectively to the edge plasma, the antenna and guard limiter have a strong interaction with accelerated particles. Resultantly, materials of the antenna and guard limiter are sputtered.

[ICRF and LHW] Hot spot effect: non-uniform energy dissipation of RF waves creates a localized high-temperature region. It causes release of plasma facing materials. The effect becomes particularly significant in high power long-pulse discharges.

[ICRF and ECRH] Resonance effects: when particles are accelerated above certain threshold energy, those orbits deviate from the last closed flux surface (LCFS) and collide with first wall.

Neutral Beam Injection

Interaction with first wall: high-energy neutral beams penetrate the plasma in low-density discharges and interact with first wall.

Trapped particles: high-energy trapped particles interact with first wall.

Beam divergence: different beam divergences originated in full, half and one-third energies of hydrogen atom may enhance the interaction with plasma facing components around injection port.

Summary of the particle species

Working particle

H, D, T (in the future)

Intrinsic & extrinsic impurities

- **Wall conditioning: He, Li, B, Si**
- **Vacuum condition: N, O**
- **Reciprocating Probe injection: C**
- **Guess puffing: Ne, Si, Ar**
- **High power auxiliary heating: C, Fe, Cu, Mo**
- **Giant ELMs: Mo, W ...**

Outline

- Tungsten and High-Z impurity source in EAST
- Impurity-related spectroscopic diagnostics in EAST
- Tungsten data needs and other important issues
- Relevant Activities
- Summary

Overview of tungsten spectroscopy diagnostics in EAST

ASIPP

EAST	Capability	Diagnostic
Divertor	Upper & lower div. W source – W^0 (4009Å)	Space-resolved VIS
	Upper div. W source (2D) – W^0 (4009Å, 4295Å, 5053Å) – W^{1+} (4218Å, 4348Å)	Space-resolved VIS (2D)
SOL (ρ=1.0-1.05)	W influx (W^{3+}-W^{6+}: 500-1500Å)	VUV survey
	W influx (W^{3+}-W^{6+}: 200-500Å)	EUV survey
Pedestal / edge	W influx & density – W^{7+}-W^{20+}: 150-260Å	EUV survey
Bulk plasma (ρ≤0.7)	W density profile – W^{24+}-W^{45+}: 15-140Å	Space-resolved EUV

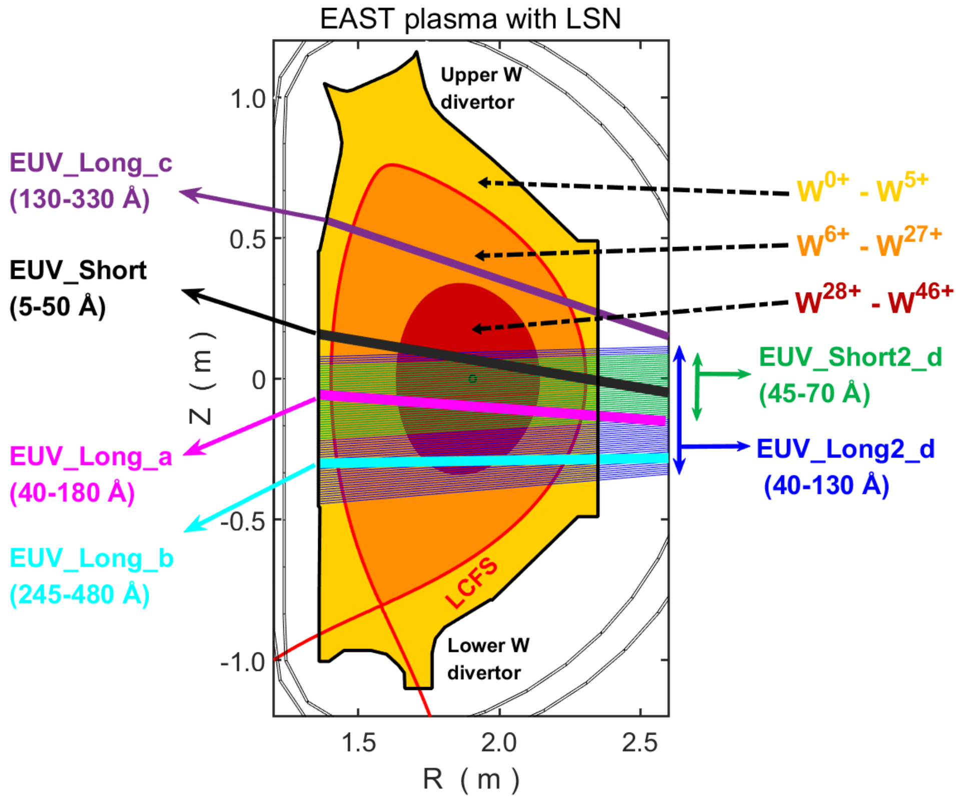

High-performance impurity spectroscopy diagnostic platform

ASIPP

Fast-time-response EUV spectrometers

(5ms/frame, 5-500Å, W^{3+}-W^{45+})

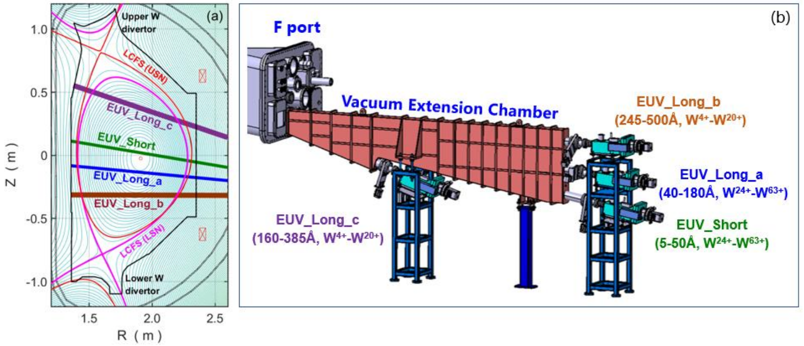

		EUV_Short	EUV_Long_a	EUV_Long_c	EUV_Long_b
λ	Capability	5-138 Å	20-500 Å		
	Operation	5-50 Å	40-180 Å	160-385 Å	245-500 Å
Ions		He^{+}, Li^{+}-Li^{2+}, C^{2+}-C^{5+}, O^{2+}-O^{7+}, Ne^{+}-Ne^{9+}, Si^{4+}-Si^{11+}, Ar^{9+}-Ar^{15+}, Fe^{4+}-Fe^{23+}, Cu^{9+}-Cu^{28+}, Mo^{4+}-Mo^{31+}, W^{3+}-W^{63+}, …			

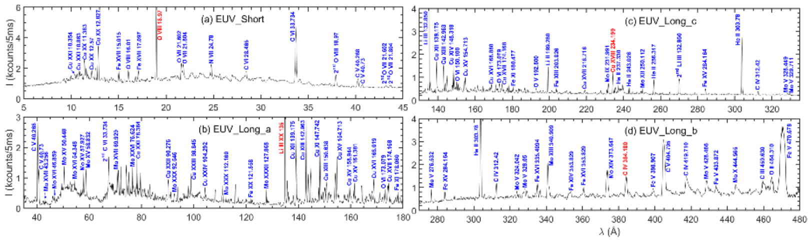

- ✓ 张文敏，**物理学报** 71, No. 11 (2022) 115203
- ✓ W.M Zhang **Phys. Scr.** 97 (2022) 045604
- ✓ W.M. Zhang **Phys. Scr.** *2024 (accepted)*

Space-resolved EUV spectrometers

(15-200ms/frame, 5-500Å, ΔZ=90cm (ρ≤0.7))

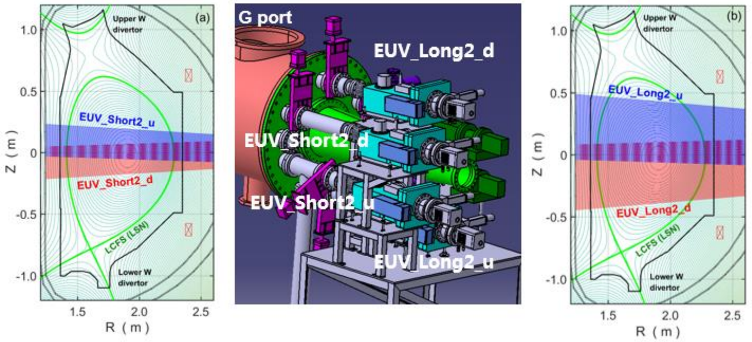

	λ range	Temporal Reso.	Spatial Reso.	Viewing range	Detector
EUV_Short2	5-130 Å	15 ms/frame	≥0.3 cm	±25 cm	CMOS
EUV_Long2	30-520 Å	200 ms/frame	≥0.8 cm	±45 cm	CCD
Ions (ρ≤0.7)	W^{24+}-W^{63+}, Mo^{24+}-Mo^{31+}, Cu^{19+}-Cu^{26+}, Fe^{18+}-Fe^{23+}…				

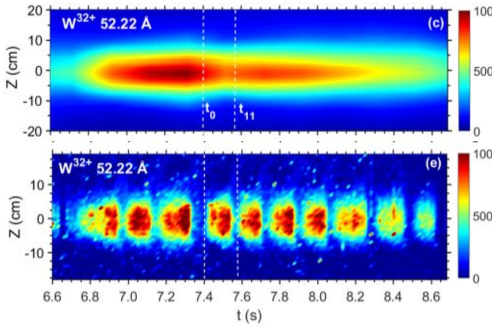

200 ms/frame

15 ms/frame

- ✓ Y.X. Cheng ***Rev. Sci. Instrum.*** 93 (2022)123501
- ✓ Y.X. Cheng ***Nuclear Ins. and Methods in Physics Research, A*** 1057 (2023) 168714

Space-resolved VIS spectrometers

(1D: ΔZ=140cm; 2D: 10x11, div. & edge)

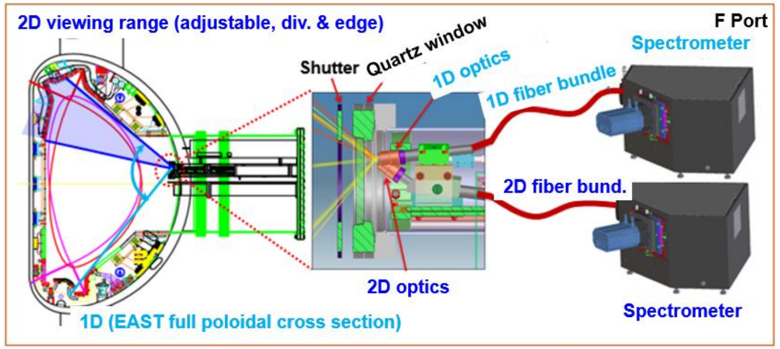

- **Endoscopic optics**
  - 2D at upper divertor: 85 x 38 cm^2 (poloidal x toroidal, remote controllable)
  - 1D full radial profile: ΔZ=145 cm
- **Fiber bundles**
  - 2D: 11 x 10 (50/62.5 μm)
  - 1D: 60 (115/125μm)
- **Quartz window for viewing port**
- **Shutter with supersonic motor**
- **Spectrometers (MK-300)**
  - Entrance slit: 0.01-4.0mm
  - Gratings: 2400, 1200, 300 g/mm
- **Detector: Andor Marana CMOS**
  - 2048 x 2048 pixel,
  - 11μm, 22.53 x 22.53 mm

Tungsten & Impurity	Deuterium
W^{0}, W^{+}, C^{2+} source – 1D & 2D, 1200/2400 g/mm	D_β/D_γ… during detachment – 1D & 2D,1200 g/mm
M1 transition from W^{7+}-W^{28+} – 1D, 1200 g/mm	D_2 Fulcher-α band – 2D,1200/2400 g/mm
Edge Impurity survey at 300-800nm – 1D & 2D, 300 g/mm	Verification of div. conf. （Snowflake, Fish tail） – 2D, 300/1200 g/mm
Edge impurity flow from Doppler shift – 2D, 2400 g/mm	DB, DW molecular ?
VB, Z_{eff} profile → EUV calibration – 1D, 1200 g/mm	

- ✓ A.L. Hu 43rd *ITPA-DG* 2023
- ✓ L. Zhang 44th *ITPA-DG* 2023

Emission lines from W^{22+}-W^{45+} in bulk plasma

ASIPP

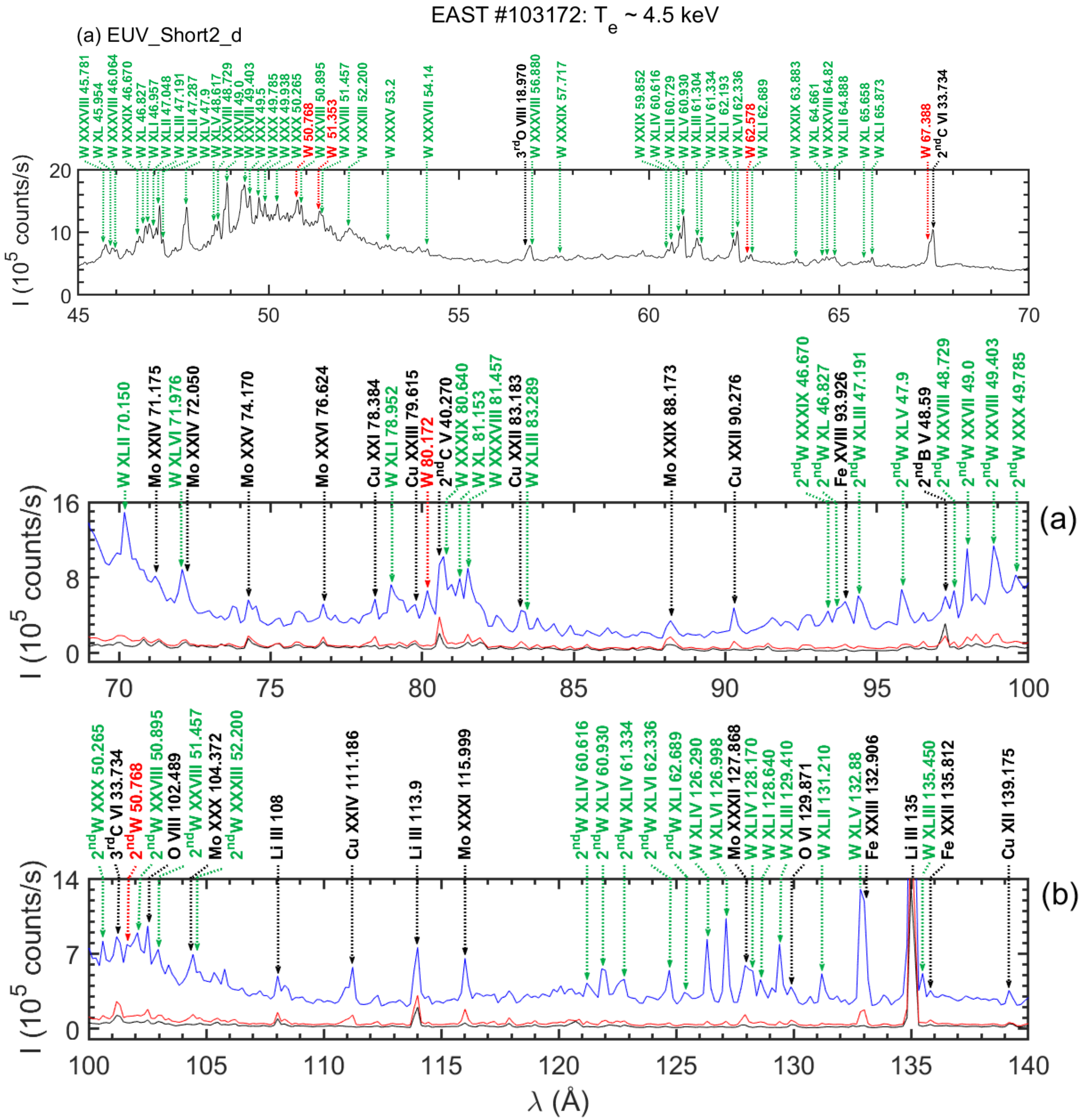

- 78 lines from W^{22+} - W^{45+} ions existed in **bulk plasma** are observed **at 10-140 Å**
- Several strong, isolated lines and W-UTAs are candidates for **tungsten transport** study

✓ W.M. Zhang *et al.*, **Spectroscopic analysis of tungsten spectra in extreme-ultraviolet range of 10-480 Å observed from EAST tokamak with full tungsten divertor** (*submitted to Physica Scripta*)

Emission lines from W^{3+}-W^{20+} ions at plasma edge

ASIPP

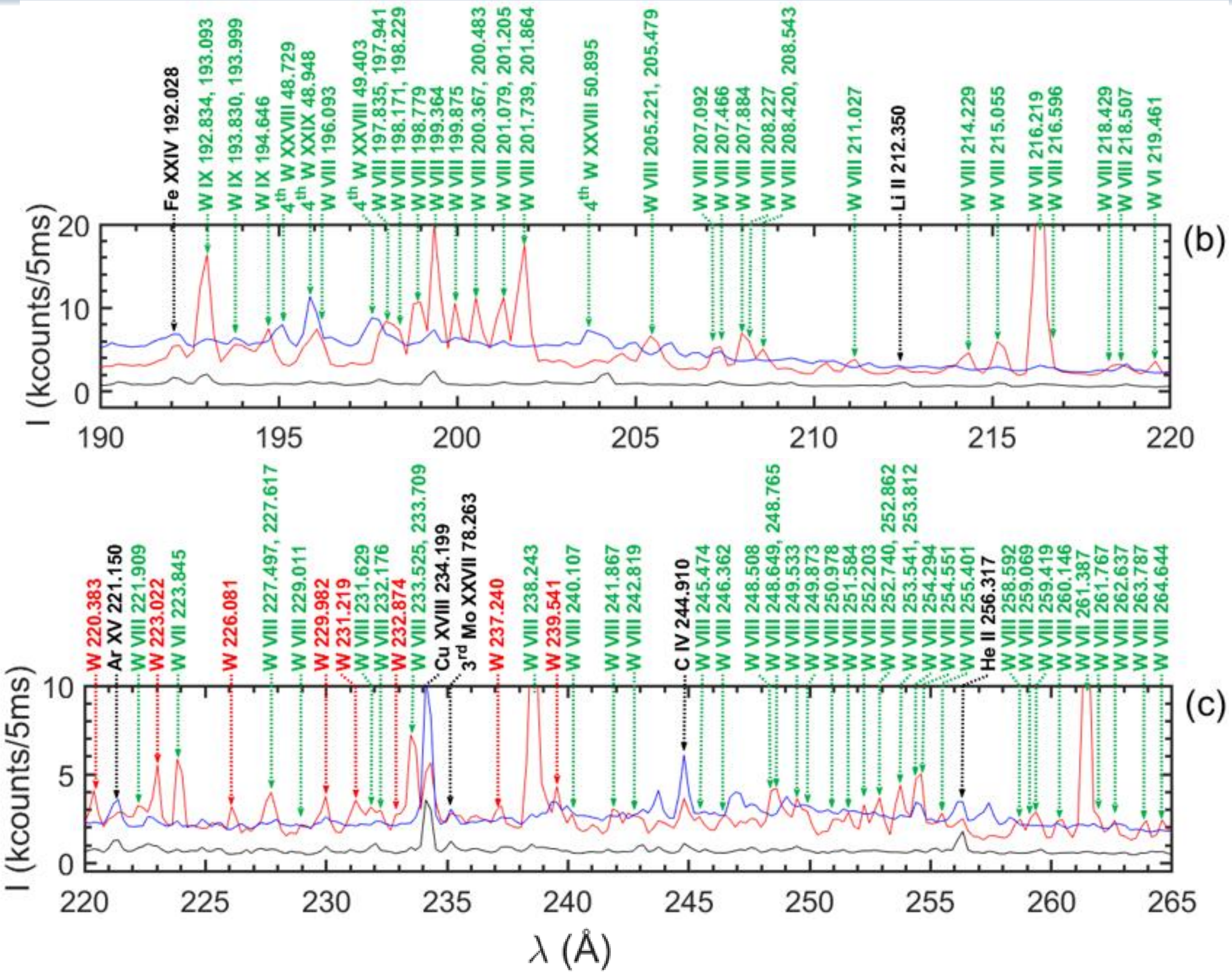

- 89 lines from **W^{3+} - W^{20+}** ions existed in **plasma edge** are observed **at 140-480 Å**
- **52 new lines** are found, probably from **W^{4+} - W^{41+}** ions
- Several strong, isolated lines and W-UTAs are candidates for **tungsten transport** study

✓ W.M. Zhang *et al.*, **Spectroscopic analysis of tungsten spectra in extreme-ultraviolet range of 10-480 Å observed from EAST tokamak with full tungsten divertor** (*submitted to Physica Scripta*)

Observation W ion distribution helps to confirm line identification

- Observation of vertical line intensity profiles of EUV spectra from various tungsten ions.
- Different peak positions indicate different W charged states (**W-UTA @T_{e0}=4.5keV**).

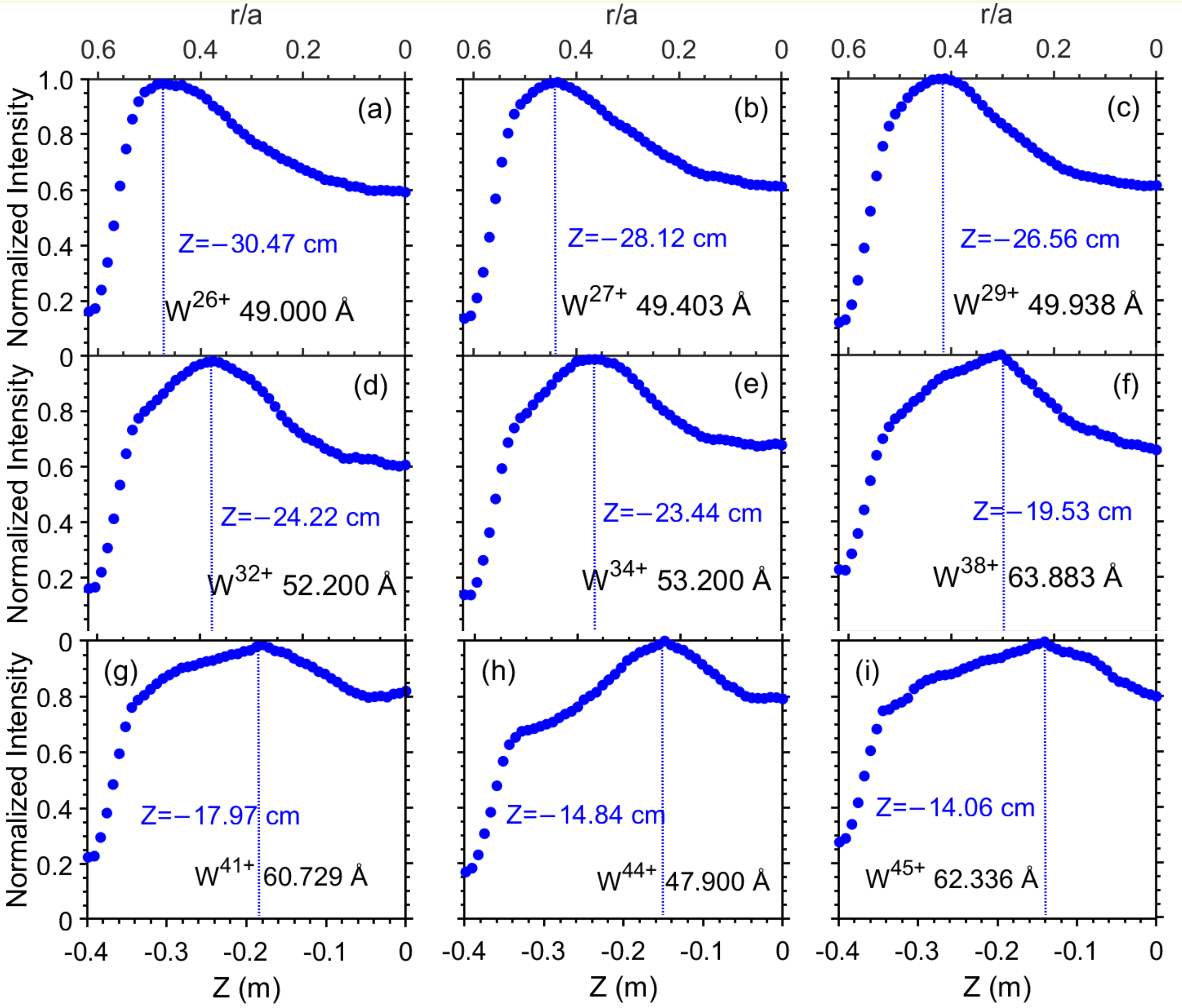

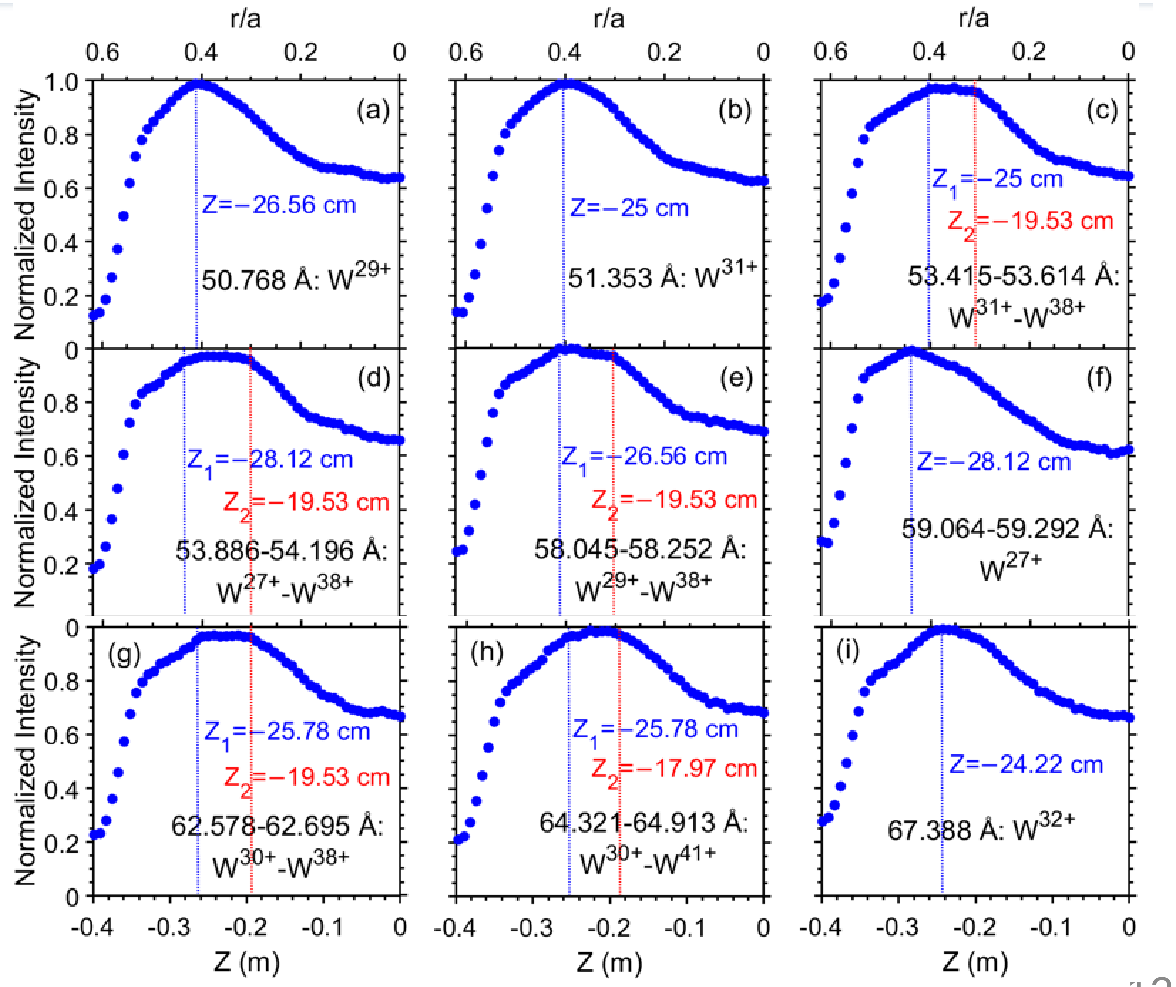

Accumulation of emission line database of Mo

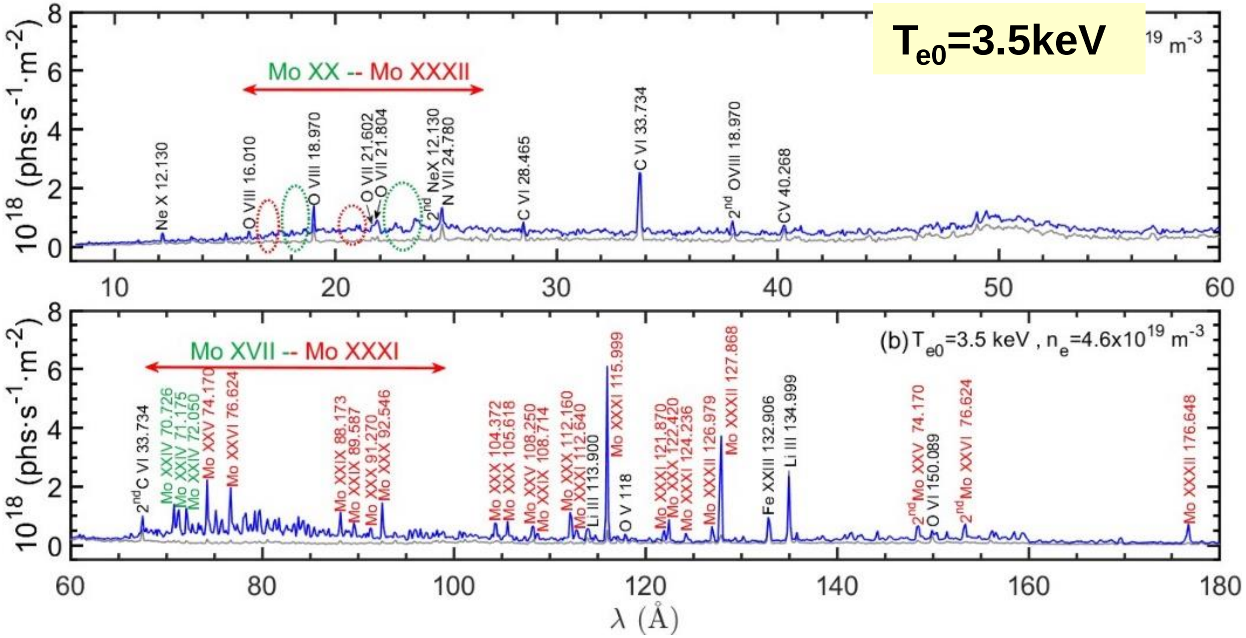

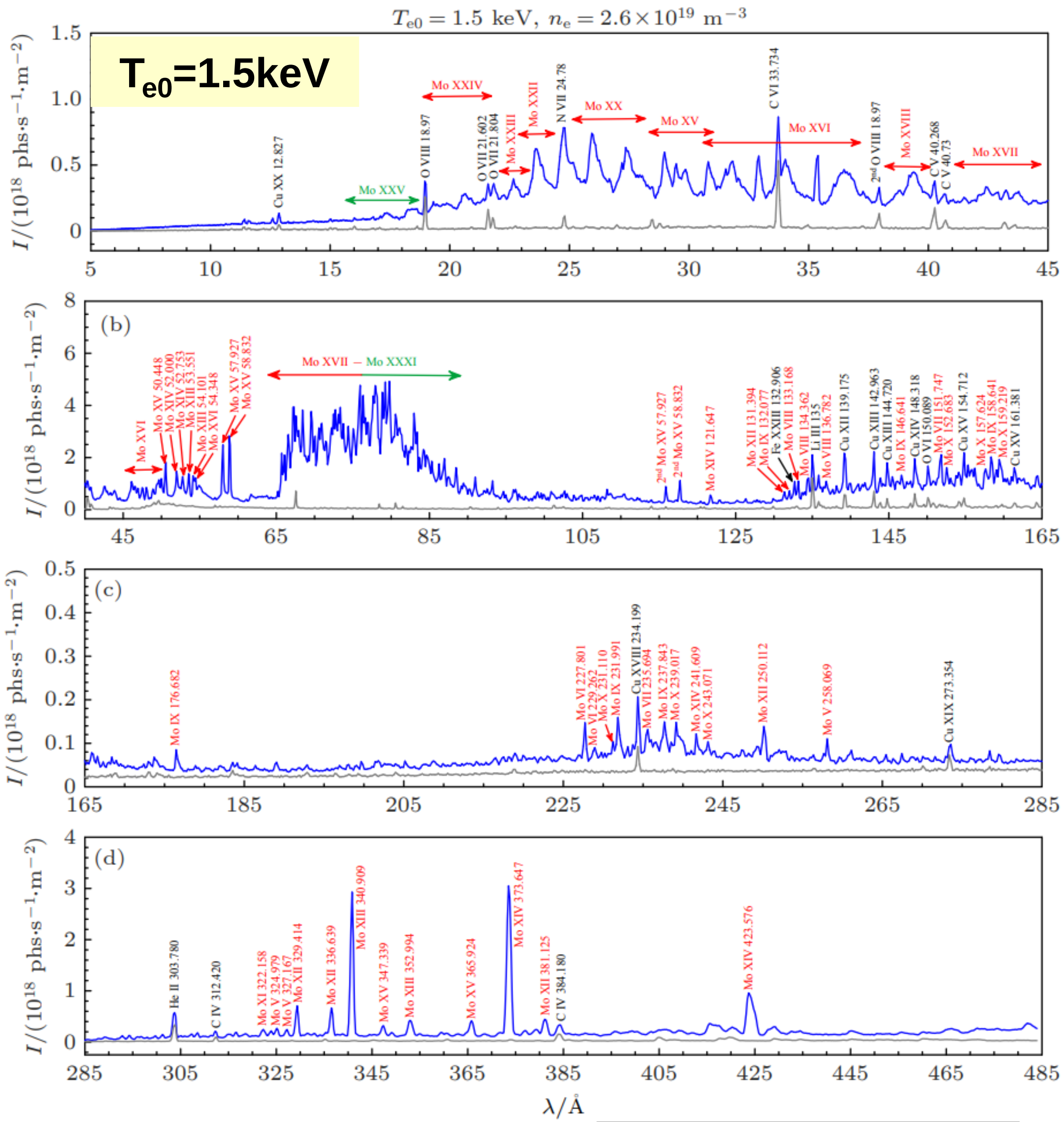

- ✓ Line emissions from Mo^{24+} - Mo^{31+} (E_i=1263-1791 eV)
- ✓ Line emissions from Mo^{4+} - Mo^{23+} (E_i=54-1082 eV)
- ■ Mo-UTA from Mo^{14+}-Mo^{24+} at 15-45 Å
- ■ Strong Mo-UTA at 65-90 Å
- ■ Isolated lines from Mo^{16+}-Mo^{31+} at 70-130 Å,
  e. g. Mo^{30+} at 116 Å, Mo^{31+} at 127.868, 176.648 Å

✓ W.M Zhang Phys. Scr. 97 (2022) 045604

✓ 张文敏 物理学报 2022

Accumulation of emission line database of Cu and Fe

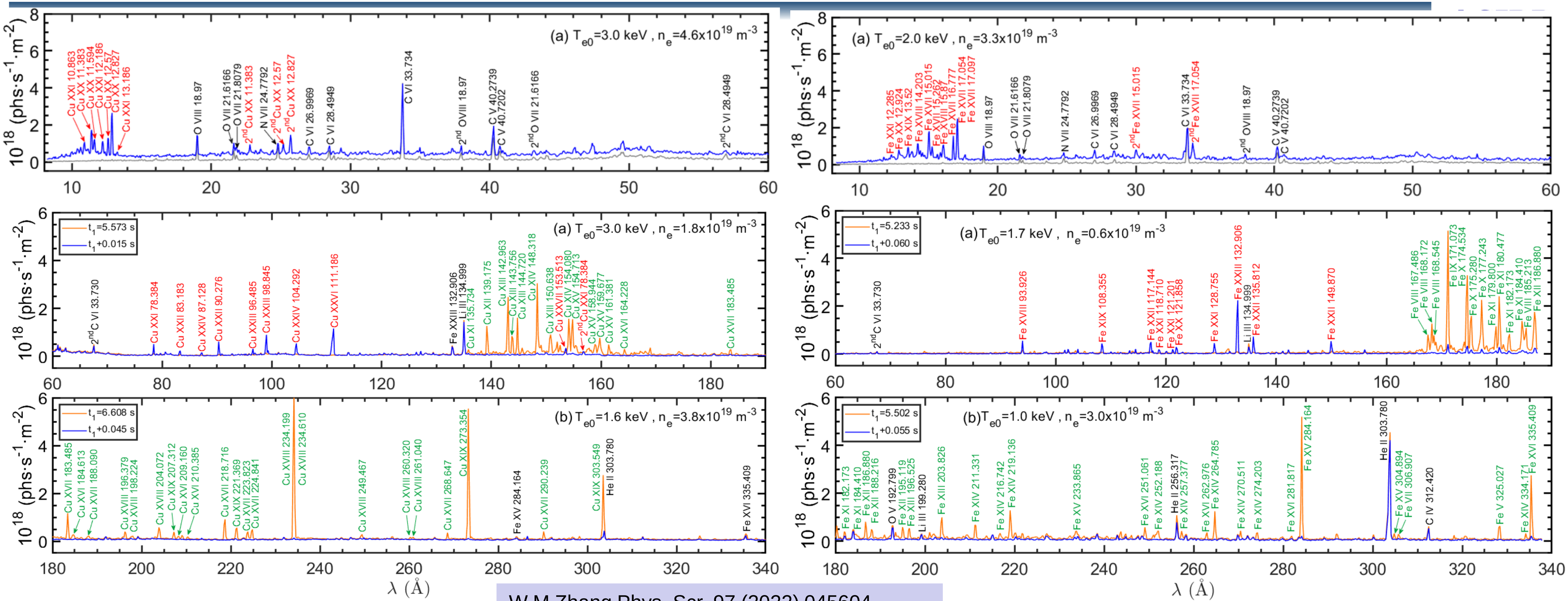

W.M Zhang Phys. Scr. 97 (2022) 045604

- ✓ Cu^{19+} - Cu^{26+} (E_i=1691-2587 eV)
- ✓ Cu^{9+} - Cu^{18+} (E_i=232-671 eV)
- ■ Cu^{19+} - Cu^{20+} at 10-14 Å, Cu^{21+} - Cu^{25+} at 80-110 Å
- ■ Cu^{10+} - Cu^{15+} at 130-165 Å, Cu^{16+} - Cu^{18+} at 180-305 Å

- ✓ Fe^{16+} - Fe^{23+} (E_i=1263-2046 eV)
- ✓ Fe^{4+} - Fe^{15+} (E_i=175-489 eV)
- ■ Fe^{16+} - Fe^{20+} at 12-17 Å, Fe^{17+} - Fe^{21+} at 90-150 Å
- ■ Fe^{7+} - Fe^{14+} at 170-285 Å, Fe^{4+} - Fe^{6+} at 300-450 Å

Outline

ASIPP

- Tungsten and High-Z impurity source in EAST
- Impurity-related spectroscopic diagnostics in EAST
- Tungsten data needs and other important issues
- Relevant Activities
- Summary

Key role of W atomic data in fusion plasma

Effective W atomic data essential for quantitative analysis

- **W cooling rate (L_W)**
  - Cooling effect of W → P_{rad} → Fusion Power balance
    - **W concentration (C_W)** evaluation with observation of P_{rad}
    - **P_{rad}(W)** with certain C_W
  - Cooling effect of W → change T_e gradient → W transport (accumulation)

- **Photo Emissivity Coefficient (PEC^{Wq+})**
  - Evaluation of **C_W using single W line** (with known fractional abundance)
  - W ion density profiles in bulk plasma ($n_{Wq+}(r)$, **W^{24+}- W^{63+}**)

- **Ionization Event per Emitted Photo (S/XB^{Wq+})**
  - Evaluation of **W influx in divertor (W^0, W^+, W^{2+})**
  - Evaluation of **W influx at plasma edge (~ W^{3+} - W^{20+})**

Periodic H-L back transition

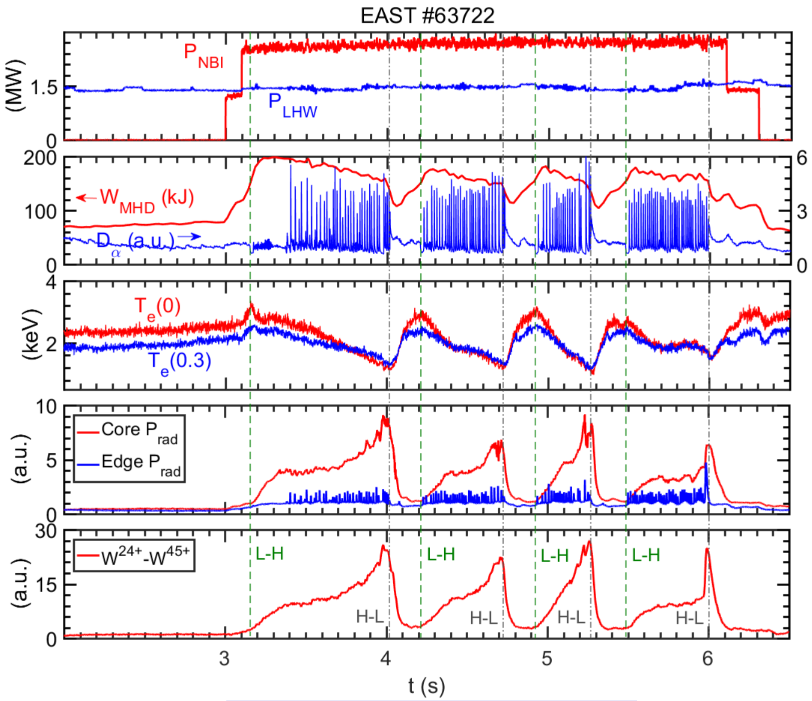

L Zhang 2nd CFEC 2021

- Cooling rate (Radiation power coefficient)

$$L_W(T_e,n_e) = \sum_q L_W^{q+}(T_e,n_e)N_{W^{q+}}/N_W$$

- Radiation power loss by W

$$P_W = \int L_W(T_e,n_e)n_e(r)\,n_W(r)\mathrm{d}V$$

- Evaluation of c_W from chord-integrated line intensity, e. g. I^{W44+}-I^{W45+}

$$I^{W^{q+}} = \int n_{W^{q+}}(l)\mathrm{PEC}^{W^{q+}}(l)n_e(l)\mathrm{d}l$$

$$= \int c_W(l)n_e(l)FA^{W^{q+}}(l)\cdot PEC^{W^{q+}}(l)n_e(l)dl$$

$$= \int c_W f_{c_W}(l)n_e(l)FA^{W^{q+}}(l)\cdot PEC^{W^{q+}}(l)n_e(l)dl$$

$$c_W = I^{W^{q+}}/\int f_{c_W}(l)FA^{W^{q+}}(l)PEC^{W^{q+}}(l)n_e^2(l)dl$$

$$\Gamma = n_e S_\sigma \int \frac{\epsilon_{jk}(\xi)}{A_{jk}n_e\mathcal{F}_{j\sigma}}d\xi = \frac{S_\sigma}{A_{jk}\mathcal{F}_{j\sigma}} \times \int \epsilon_{jk}(\xi)\,d\xi$$

$$\Gamma = \frac{S_\sigma}{A_{jk}\mathcal{F}_{j\sigma}} \times \int \epsilon_{jk}(\xi)\,d\xi \equiv \mathcal{SXB}_{jk} \times \int \epsilon_{jk}(\xi)\,d\xi$$

$$= \mathcal{SXB}_{jk} \times I_{jk}$$

$$\mathcal{SXB}_{jk} = \frac{\Gamma}{I_{jk}} = \frac{S_\sigma}{A_{jk}\mathcal{F}_{j\sigma}}$$

Limited application of W atomic data in quantitative analysis

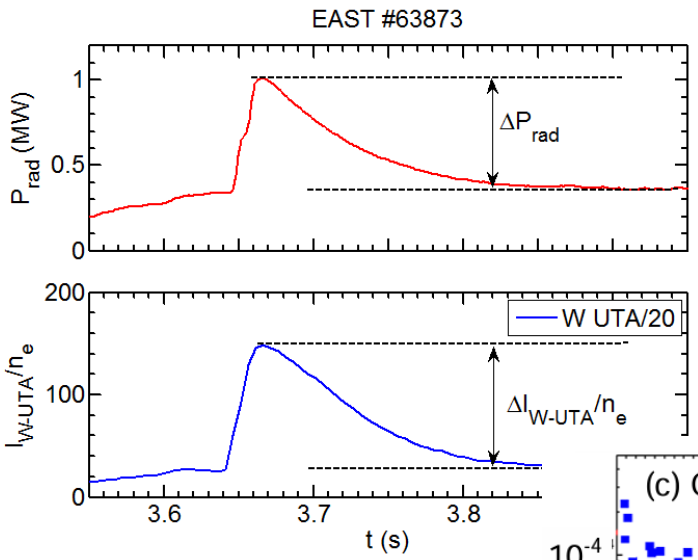

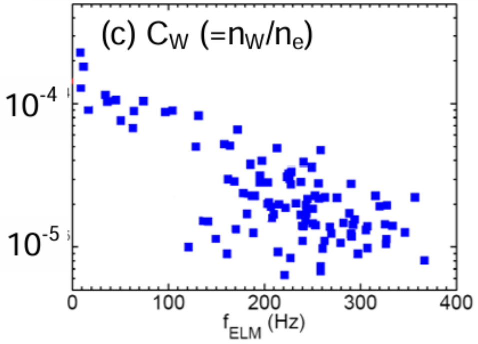

- For calibration shot:

$$L_W^{Cali} = \Delta P_{rad}^{Cali} / (\Delta I_{W-UTA}^{Cali}/n_e)$$

- For target shot:

$$P_W = L_W^{Cali} \cdot (I_{W-UTA}/n_e) = \int L_W(T_e, n_e) n_e(r)\, n_W(r) \mathrm{d}V$$

$$= \int L_W(T_e, n_e) n_e^2(r)\, c_W f_{cW}(r) \mathrm{d}V$$

$$c_W = L_W^{Cali} \cdot (I_{W-UTA}/n_e) / \int L_W(T_e, n_e) n_e^2(r)\, f_{cW}(r) \mathrm{d}V$$

c_W (r): density profile of W, $c_W(r) = c_W \cdot f_{cW}(r)$
$f_{CW}(r)$: normalized density profile of W
I_{W-UTA}: chord-integrated intensity of W-UTA at 45-70Å

- **Quantitative analysis limited in**
  - W concentration evaluated from W-UTA at ~50 Å → **W cooling rate + P_{rad}**
  - Divertor W source from W^0 (4009 Å) → **SXB (W^0)**
  - W ion density profiles in bulk plasma → **PEC (W^{43+}-W^{45+})**

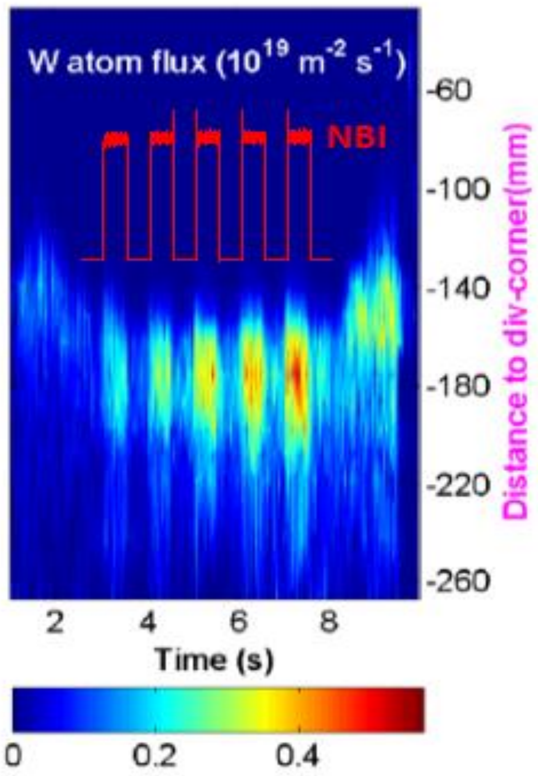

H.M. Mao ***Rev. Sci. Instrum*** 88, 043502 (2017)

Vertical profile: $I^{W^{q+}}(Z)$

↓ EFIT equilibrium, Abel Inversion

Local emissivity profile: $\varepsilon^{W^{q+}}(r)$

↓ $T_e(r)$, n_e (r), **PEC(T_e,n_e)**

Density profile: $n^{W^{q+}}(r)$

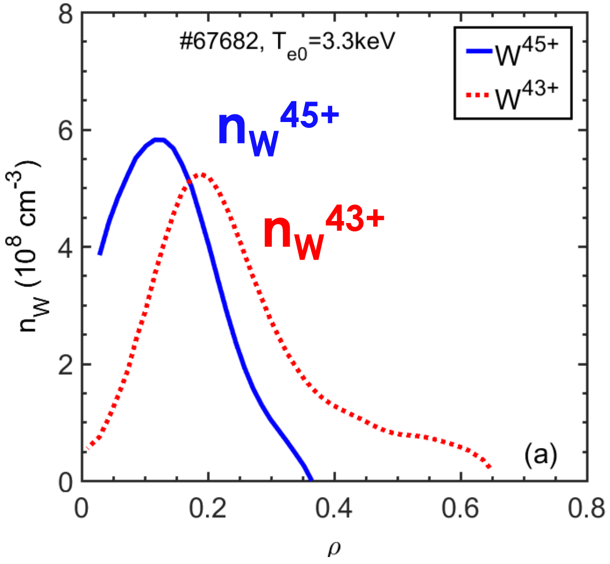

Other important / fundamental issues

ASIPP

- **Absolute intensity calibration in EUV and X-ray range**
  - Calculation of bremsstrahlung radiation intensity using Z_{eff} from VB
  - Enough number of line pairs
- **Calculation of energy-resolved radiation in full range**
  - For calibration of Soft X-ray imaging and bolometer system
- **High ionization stage W ions toward future burning plasma**
  - Observation of emission lines from Wq+ with q>45
  - PEC data for these lines
- **Low ionization stage W ions for edge W influx**
  - Observation of emission lines from Wq+ with q=3-20
  - S/XB data for these lines

Outline

ASIPP

- Tungsten and High-Z impurity source in EAST
- Impurity-related spectroscopic diagnostics in EAST
- Tungsten data needs and other important issues
- Relevant Activities
  - S/XB calculation
  - Tungsten research at NWNU
  - Tungsten research at Fudan University
- Summary

S/XB calculation and influx evaluation for W^{5+} ion

ASIPP

The S/XB calculation for W^{5+} ion:

- S is obtained with a full detailed Distorted-Wave calculation, including Excitation-Autoionization up to n=13
- A and Q are from HULLAC, AutoStructure and FAC
- CRM include full levels (430 levels)
- Two metastable levels included in $F_{j,\sigma}$

✓ generates an ADF04 files, compatible with ADAS
✓ construct the population matrix
✓ solve the level population
✓ produce a synthetic spectra based on the emissivity of each line (n_j *A_{ji})

Wq+	λ (Å)		Transitions		
	This work	Database	Relative (counts/5ms)	Lower level	Upper level
W VIII (W^{7+})	201.700 ± 0.02	201.739[a]	11720[A]	$4f^{13}5p^6\ ^2F_{7/2}$	$4f^{13}5p^5 5d$ 9/2
W VII (W^{6+})	216.351 ± 0.01	216.219[b]	34550[A]	$4f^{14}5p^6\ ^1S_0$	$4f^{14}5p^5(^2P^\circ_{1/2})5d$ $(1/2,3/2)^\circ_1$
	223.836 ± 0.01	223.846[b]	5872[A]	$4f^{14}5p^6\ ^1S_0$	$4f^{14}5p^5(^2P^\circ_{3/2})6s$ $(3/2,1/2)^\circ_1$
	261.317 ± 0.01	261.387[b]	13900[A]	$4f^{14}5p^6\ ^1S_0$	$4f^{14}5p^5(^2P^\circ_{3/2})5d$ $(3/2,5/2)^\circ_1$
W VI (W^{5+})	382.133 ± 0.04	382.145[b]	661[B]	$5d\ ^2D_{3/2}$	$5f\ ^2F^\circ_{5/2}$
	394.072 ± 0.04	394.133[b]	713[B]	$5d\ ^2D_{5/2}$	$5f\ ^2F^\circ_{7/2}$
W V (W^{4+})	449.673 ± 0.05	449.649[b]	549[B]	$5d^2\ ^3P_1$	$5d(^2D_{5/2})5f\ (5/2,5/2)^\circ_2$

$$4f^{14}5f)_{5/2} \rightarrow (4f^{14}5d)_{3/2}$$ 382.13Å

$$(4f^{14}5f)_{7/2} \rightarrow (4f^{14}5d)_{5/2}$$ 394.07Å

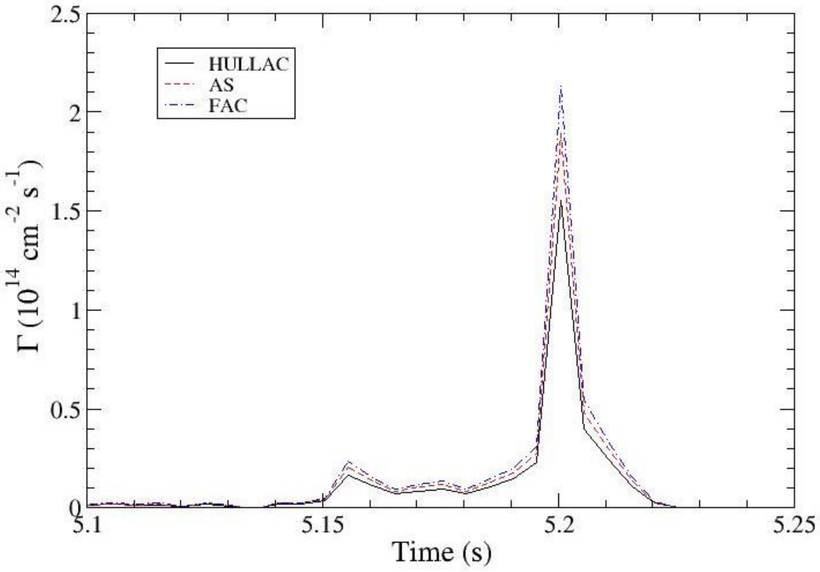

Recent Progress on Tungsten Research at NWNU

Dr. DING Xiaobin

Energy level, Radiative transition data and Spectrum		
Ding, X., Liu, Y., et al. *Phys. Lett. A*, 2022, 454, 128500.	W^{13+}	M1, VIS
Komatsu, A., Ding, X. et al. *Plasma Fusion Res.*, 2012, 7, 1201158.	$W^{8+\text{-}28+}$	UV, VIS
Minoshima, M., Ding, X. et al. *Phys. Scr.*, 2013, T156, 014010.	$W^{25+\text{-}29+}$	VIS
Ding, X., Liu, J., et al. *Phys. Lett. A*, 2016, 380, 874.	W^{26+}	VIS
Kato, D., Ding, X., et al. *Phys. Scr.*, 2013, T156, 014081.	W^{26+}	VIS
Ding, X., Murakami, I., et al. *Plasma Fusion Res.*, 2012, 7, 2403128.	W^{27+}	M1, VUV
Ding, X., Xu, Y., et al. *Phys. Lett. A*, 2024, 493, 129266.	W^{53+}	M1, VUV
Ding, X., Yang, J., et al. *Phys. Lett. A*, 2018, 382, 2321.	W^{54+}	M1, VUV
Ding, X., Yang, J., et al. *J. Quant. Spectrosc. Radiat. Transf.*, 2018, 204,7-11.	W^{54+}	Soft X-ray
Atomic Data		
Zhang, S., Ding, X., et al. *Chin. Phys. B*, 2024 , 33, 033401.	W^{8+}	CI
Ding, X., Dong, C., et al. *J. Phys. B-At. Mol. Opt.*, 2012, 45, 035003.	W^{27+}	Ag-like
Ding, X., Sun, R., et al. *Atom. Data Nucl. Data*, 2018, 119, 354.	W^{54+}	Ca-like
Ding, X., Sun, R., et al. *J. Phys. B-At. Mol. Opt.*, 2017, 50, 045004.	W^{54+}	E1,M1,E2,M2
Ding, X., Sun, R., et al. *Eur. Phys. J. D*, 2017, 71, 73.	W^{54+}	Electron Correlation
Kwon, D., Ding, X., et al. *Atom. Data Nucl. Data*, 2018, 119, 250.	W^{2+}-W^{72+}	DR
Collisional Radiative model (CRM)		
Ding, X., F. Zhang, et al. *Phys Rev A* , 2020, 101, 042509.	W^{13+} -W^{15+}	EBIT
Ding, X.,Lei, L., et al. *New J. Phys.*, 2024, 26(5): 053001.	W^{40+}-W^{42+}	EAST
Ding, X., Yang, P., et al. *Phys. Lett. A*, 2021, 420, 127758.	W^{43+} -W^{45+}	EAST

Collisional-radiative modeling of the 5p-5s spectrum of W^{13+}-W^{15+} ions

IP of W	
W^{13+}	290.7eV
W^{14+}	325.3eV
W^{15+}	361.9eV

Y. Kobayashi et al, Physical Review A, 2015 92 022510. W^{14+}

Wenxian Li et al, Physical Review A, 2015 91 062501. W^{13+}

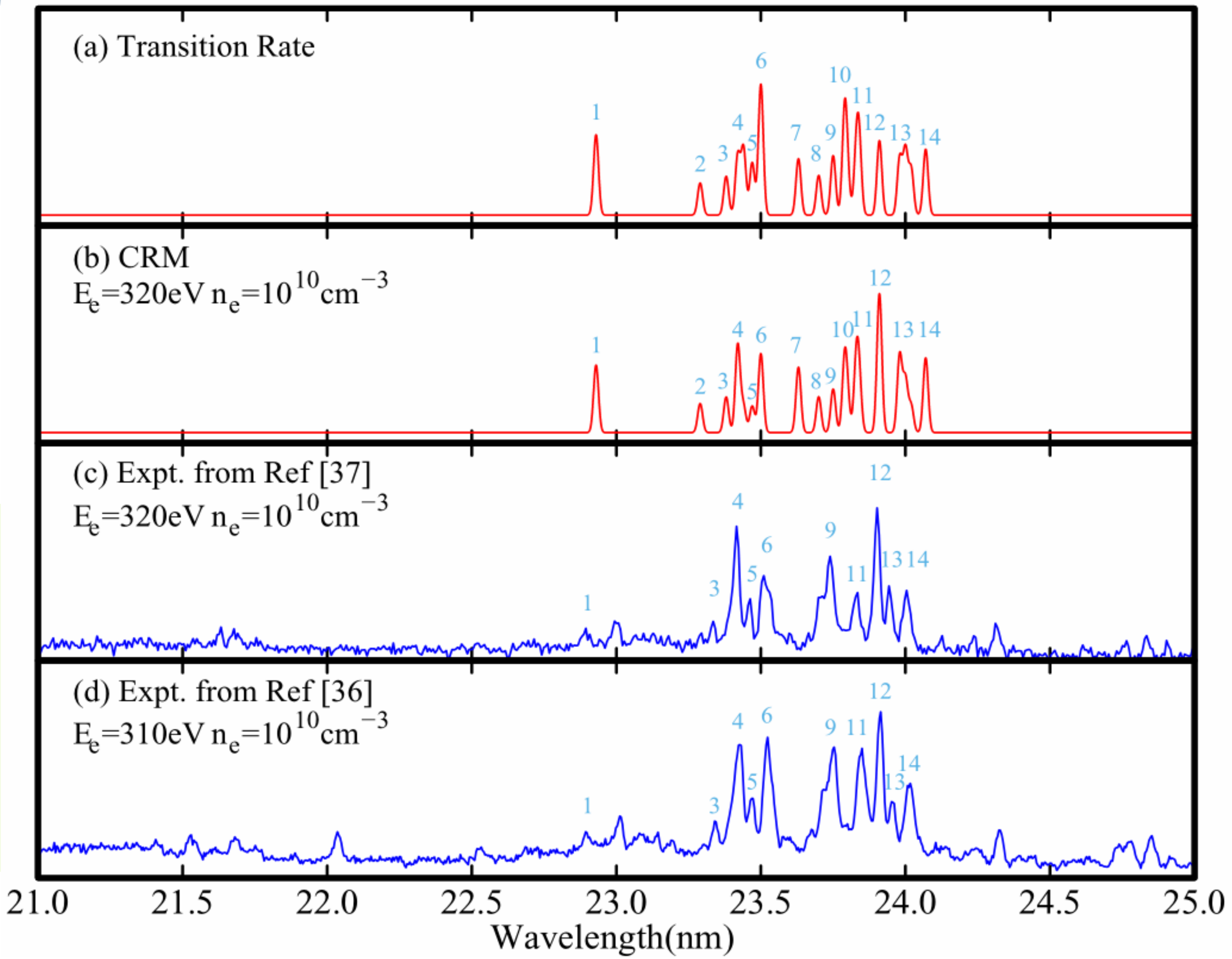

- Energy level, radiative transition rate, and collision excitational cross section are calculated by considering the electron correlation, relativistic, QED effect.
- Reasonable collisional radiative model was constructed, which helps to identify the transitions of the ions and solves the conflicition on the assignment of the ionization.

Accurate calculation on the atomic data could aid the validation and explanation on the experiment.

Ding, X., et al. ***Phys Rev A*** , 2020, 101, 042509.

Collisional-radiative modeling for the EUV spectra from W^{40+}-W^{45+} ions

Fractional Abundance

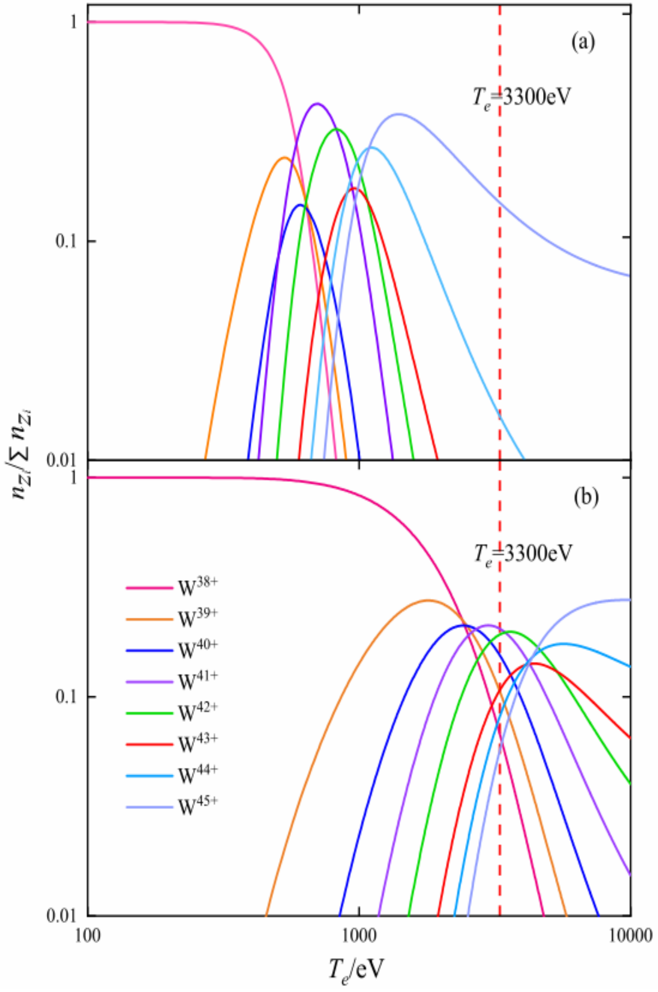

Spectrum from W^{40+}-W^{45+} ions

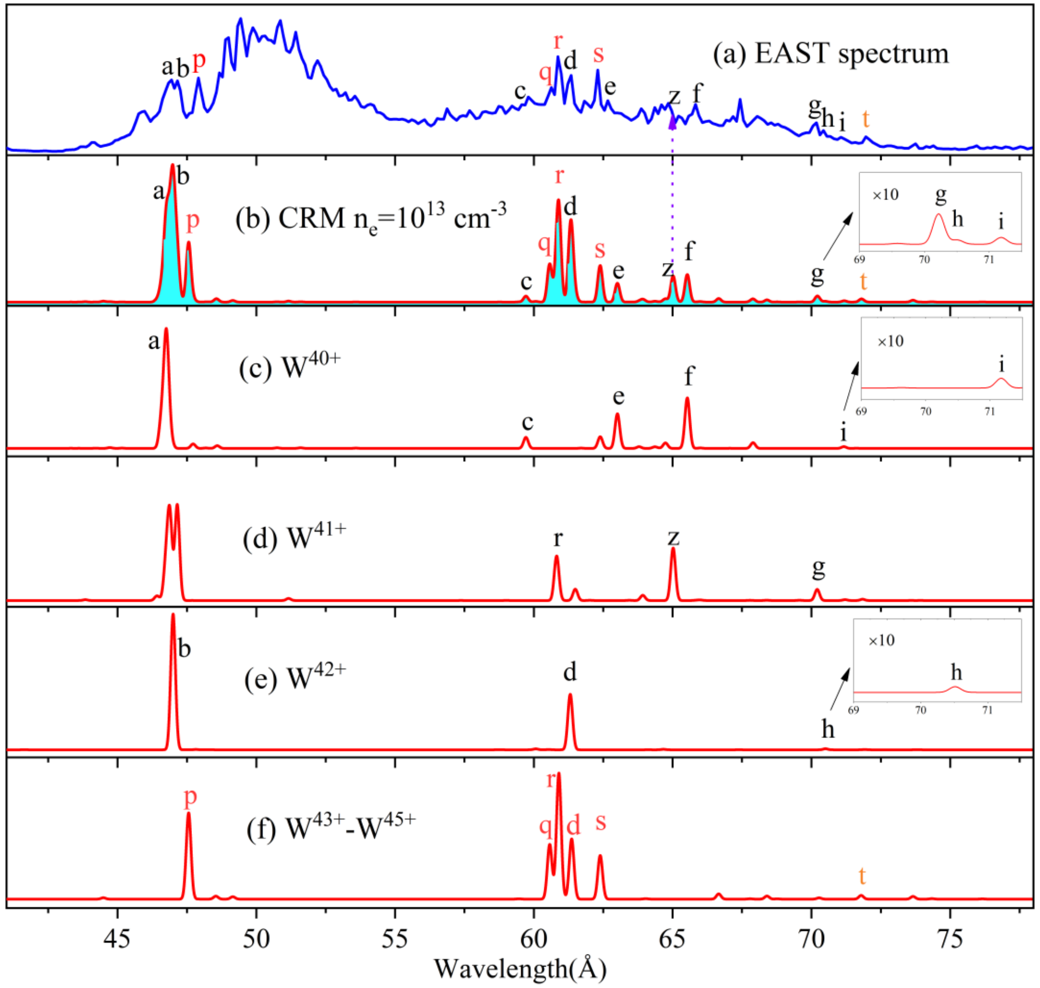

T_e Dependence

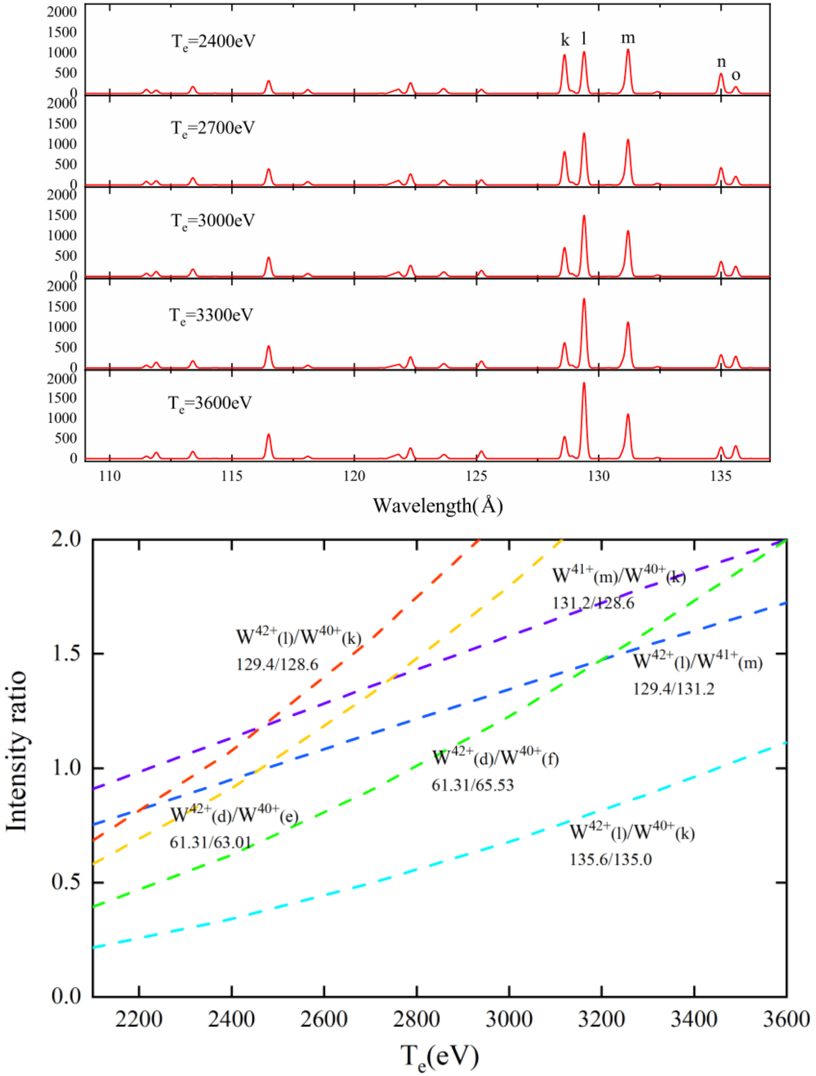

Explained the EUV spectrum of W^{40+}- W^{42+} spectra from EAST plasma by CRM @ $n_e=10^{13}$ cm^{-3}, T_e=3.3 keV

Lei, L., *et al.* ***New J. Phys.***, 2024, 26(5): 053001

Running EBITs: Shanghai-EBIT

Dr. YAO Ke

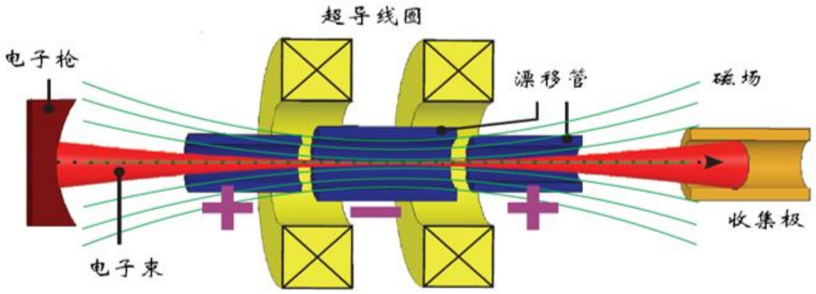

Para. Achieved	
Electron energy	0.6 - 151 keV
Electron current	215 mA
Magnetic field	4.8 T
Electron density	10^{11-12} cm^{-3}
Vacuum	7.5×10^{-11} Torr
Coolant	L-He (4.2 K)

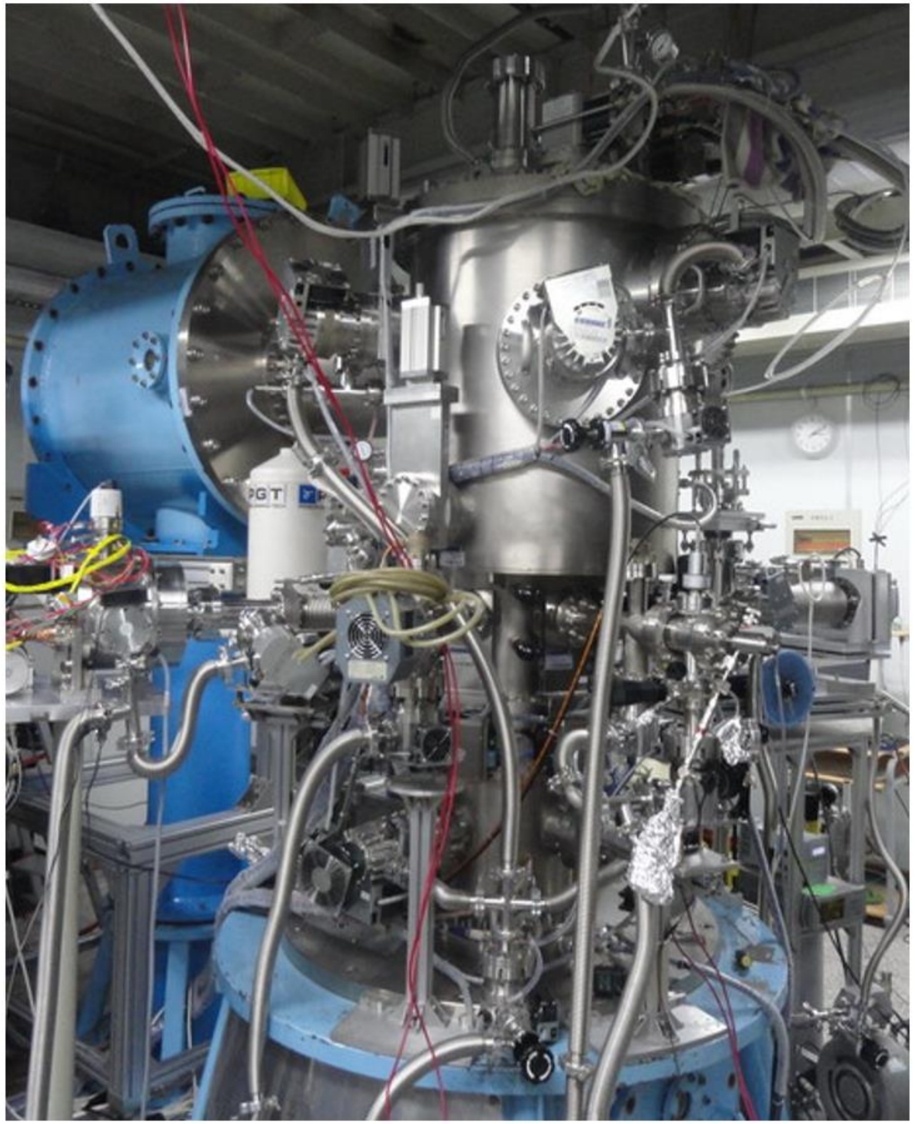

Ions produced in SH-EBIT

Elements	Charge State
H、He、C、N、O、F、Ne、S	1+…..Bare
Ar (18)	1+…..Bare
Fe (26)	1+…..Bare
Ni (28)	1+…..Bare
Kr (36)	1+…..Bare
Mo (42)	1+…..40+
Xe (54)	1+…..Bare
Ba (56)	1+…..54+
W (74)	**1+….. 72+**
Au (79)	1+….. 77+
U (92)	1+….. 84+

Running EBITs: three low energy EBITs

- ✓ High Temperature superconducting magnet: B= 0.1~0.25T
- ✓ Ee=0.03~3.0 keV
- ✓ Ie=10 mA

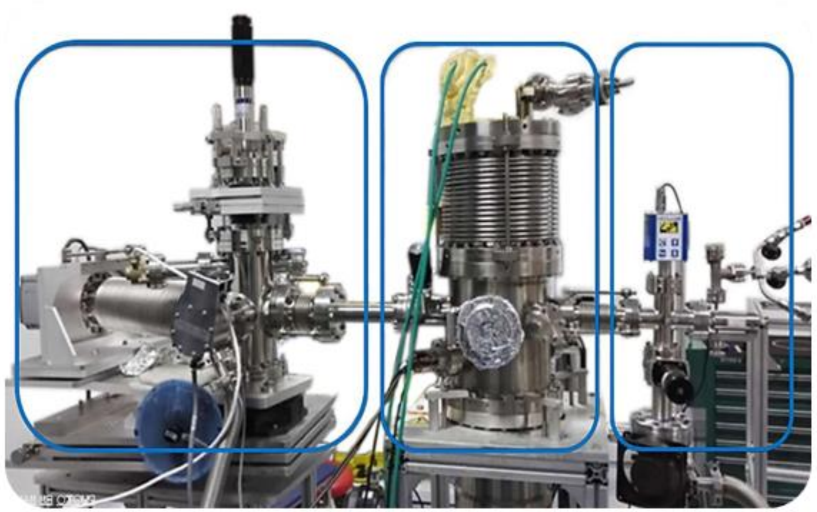

Lowest energy 30 eV

- ✓ Permanent magnet: B=0.56 T
- ✓ Ee=0.1-3.0 keV
- ✓ Ie=10 mA

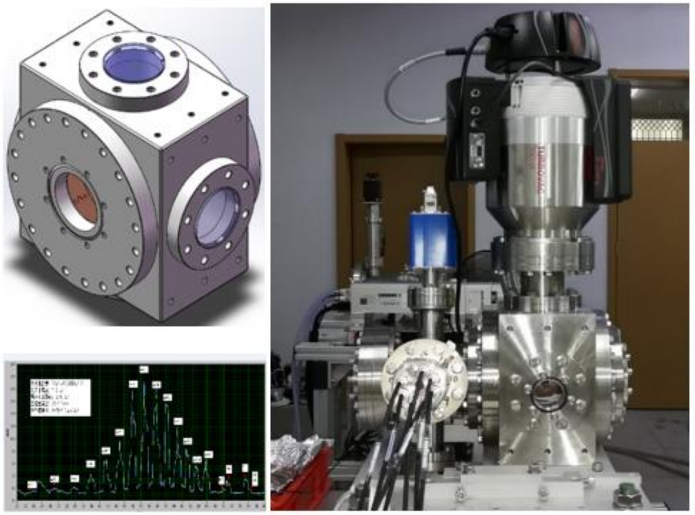

Magnet inside vacuum

- ✓ Permanent magnet: B= 0.65 T
- ✓ Ee=0.1~15 keV
- ✓ Ie=10 mA (upgrading, BaO cathode)

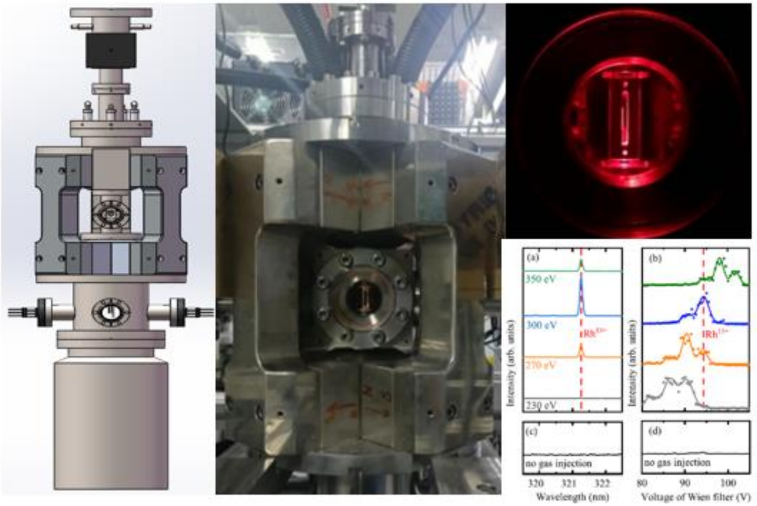

External magnet

Observation angle 42

Visible spectra to hard X-ray

W spectra observation in full wavelength range

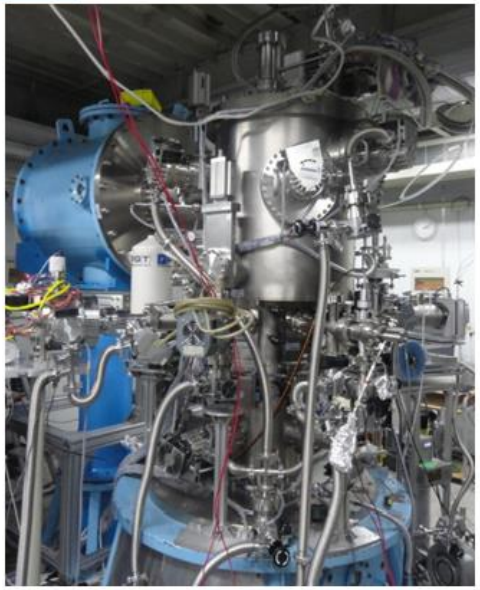

HpGe (1-200 keV)

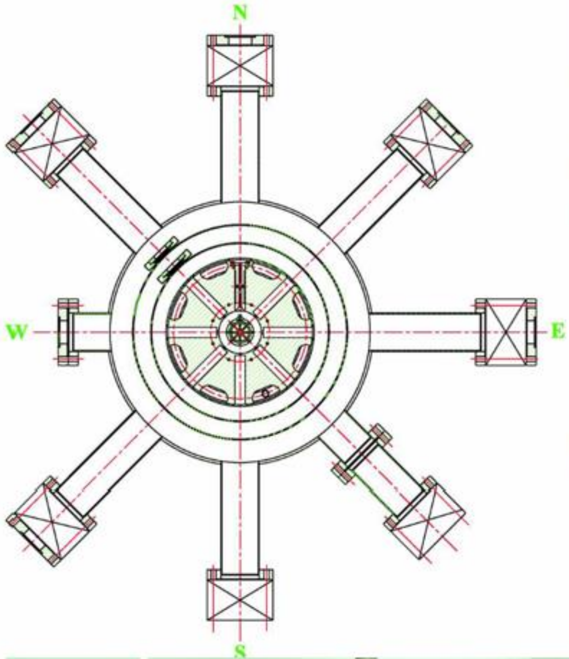

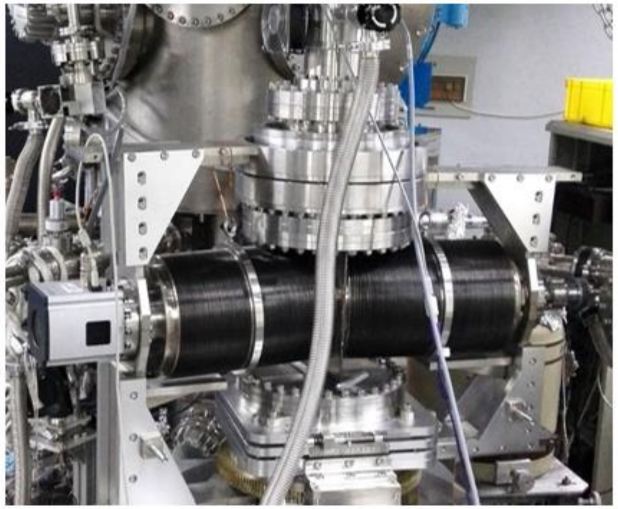

Crystal (30-1 Ǻ)

Visible to UV (10000-300 Ǻ)

EUV-I. (300-20 Ǻ)

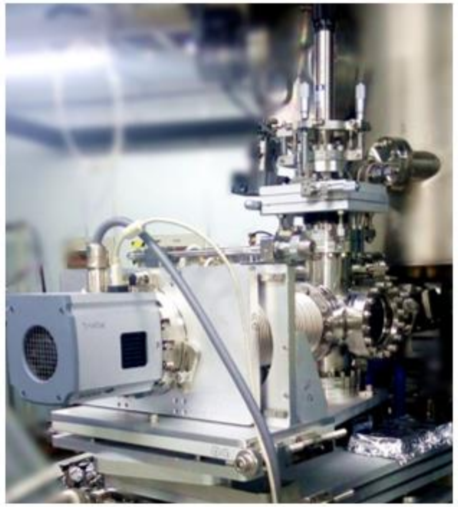

EUV-II. (300-20 Ǻ)

Recent activities on tungsten: W^{q+} spectra in Fudan University

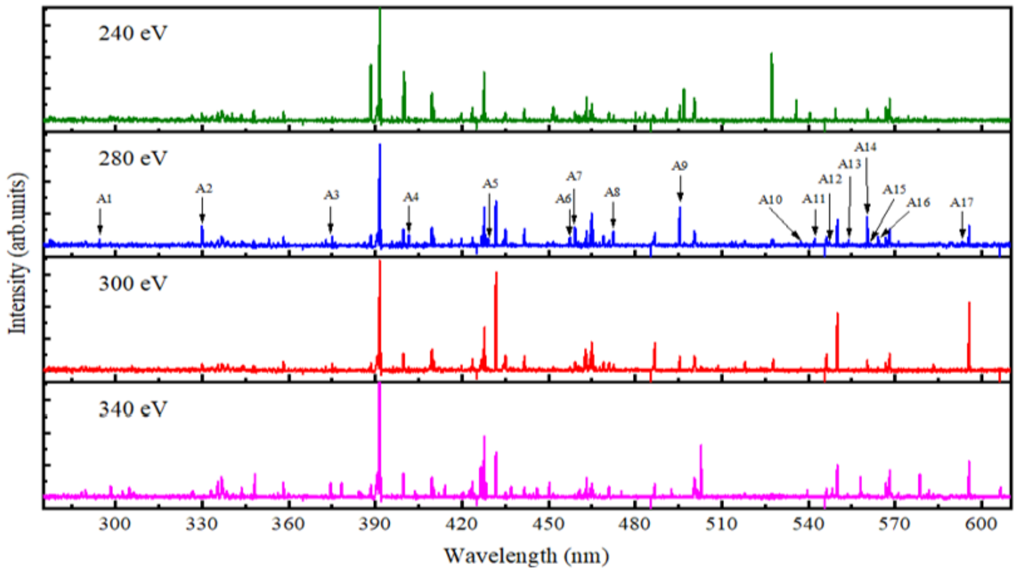

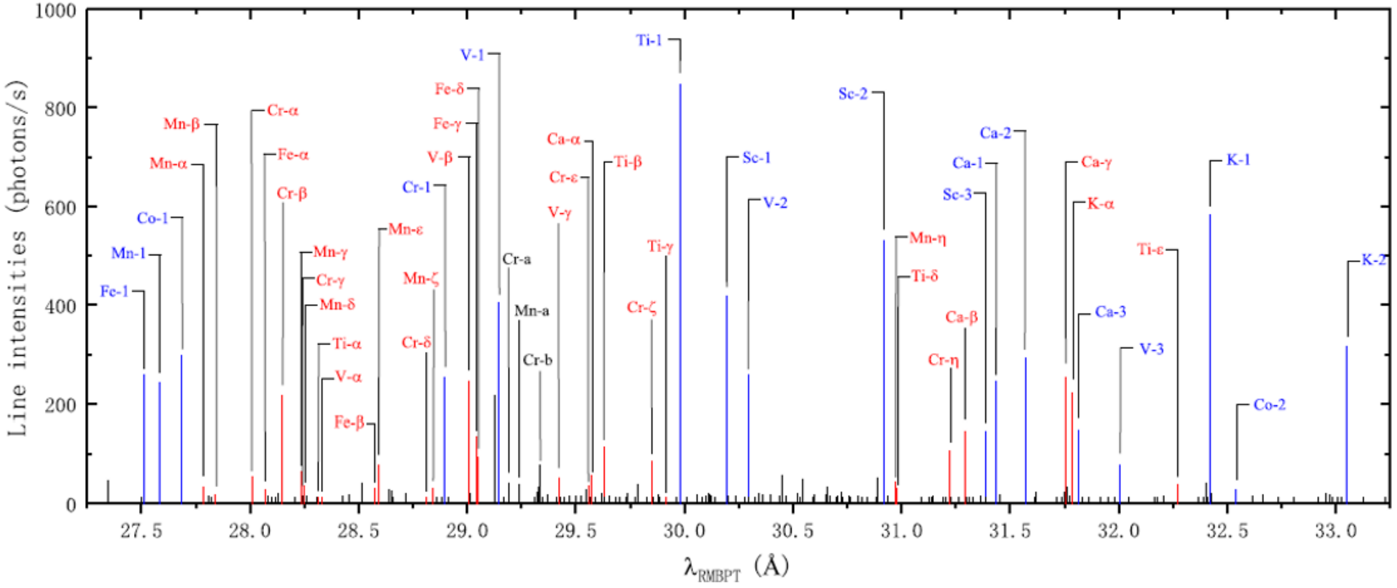

- High resolution tungsten spectra measured at EBIT.
- High accuracy atomic structure calculations:

  Relativistic Configuration Interaction (**RCI**)

  Multi-Configuration Dirac-Hartree-Fock (**MCDHF**)

  Relativistic Many-Body Perturbation Theory (**RMBPT**)

JQSRT,**262**(2021); PRA,**103**(2011), JQSRT,**279**(2022), JPB,**55**(2022), PRA,105(2022), Can. J. Phys., **102** (2024), Plasma Phys. Control. Fusion **66** (2024), JQSRT,325(2024)

Recent activities on tungsten spectra in Fudan University

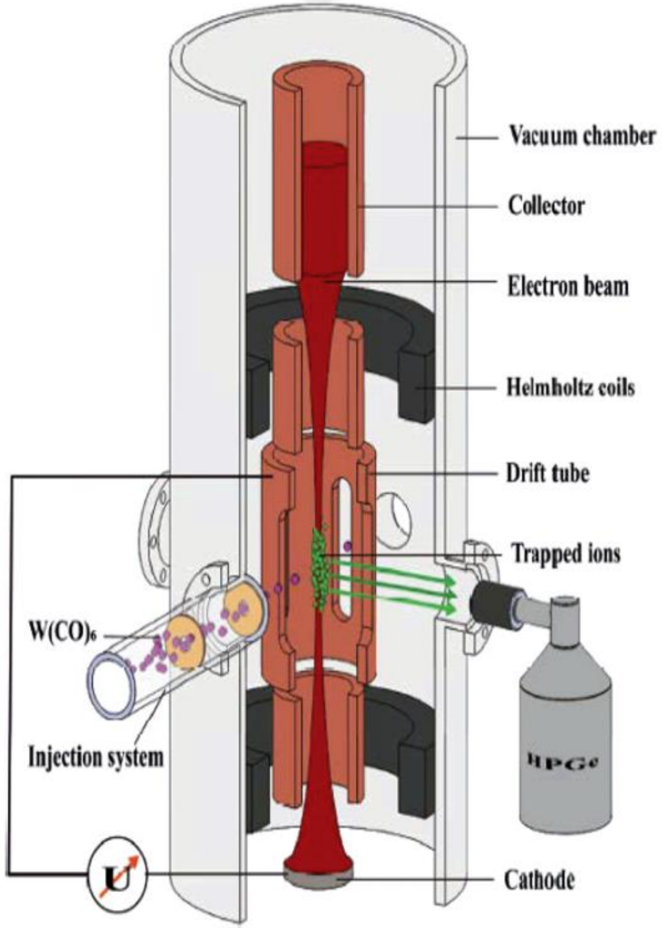

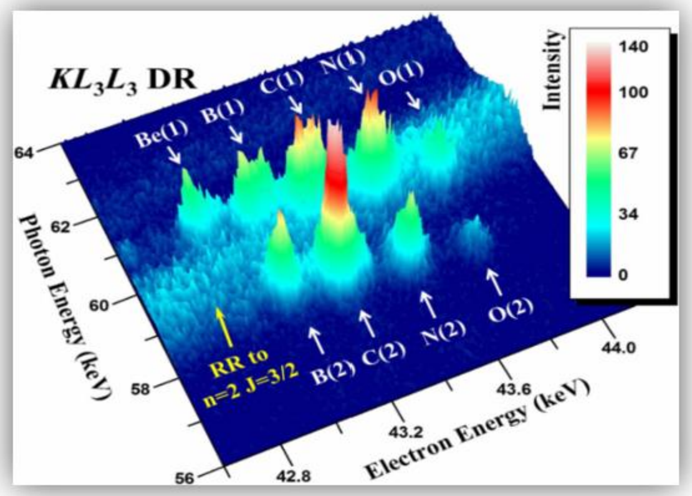

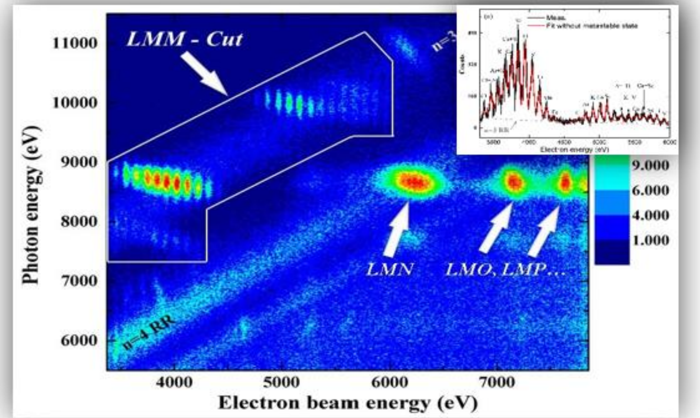

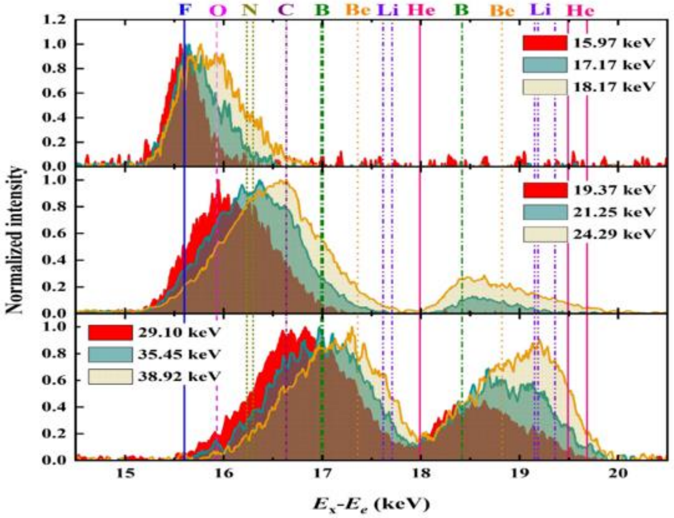

W^{65+} - W^{72+}

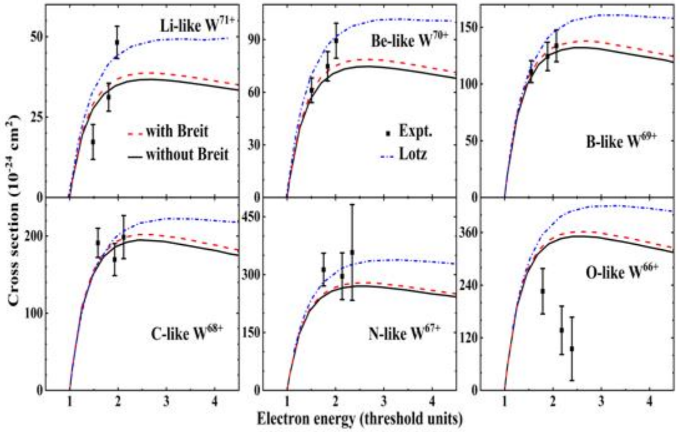

- ✓ K, L –shell excitation DR resonance strength
- ✓ Electron impact ionization cross-sections

Tu, *et al.*, PoP, **23**(2016)
Tu, *et al.*, PRA, **96**(2017)
Niu, *et al.*, Phys. Plasmas **30** (2023)

Metastable state ionization $W^{4+} \rightarrow W^{7+}$

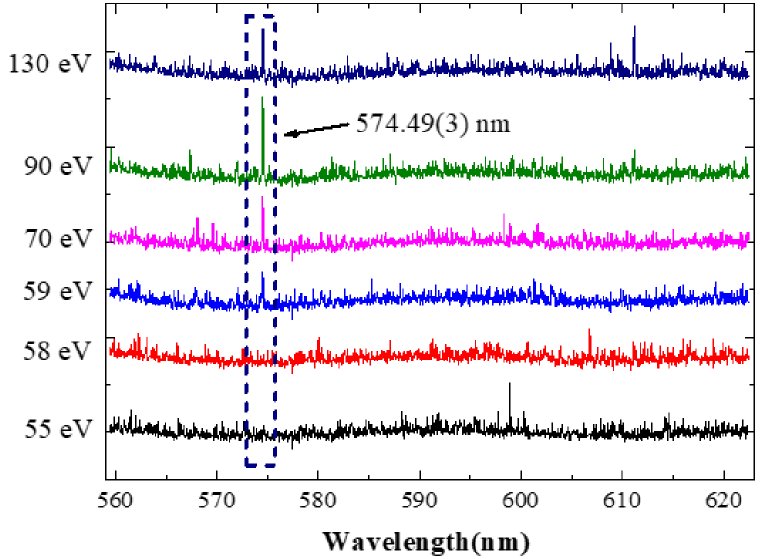

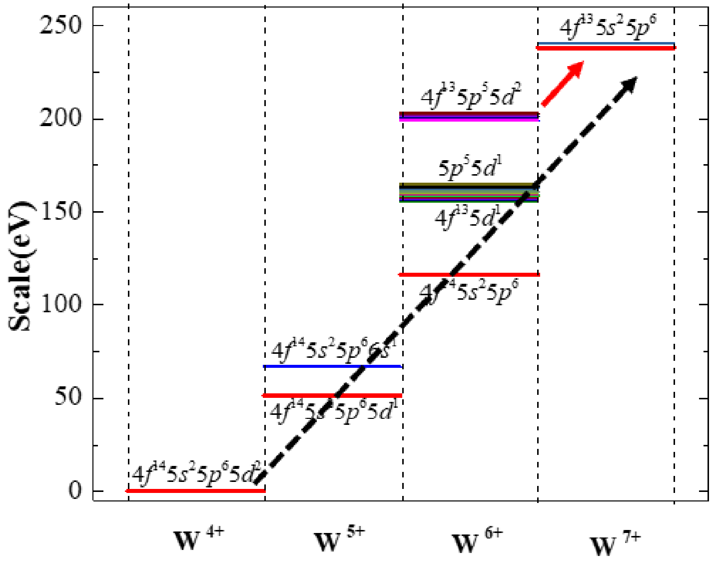

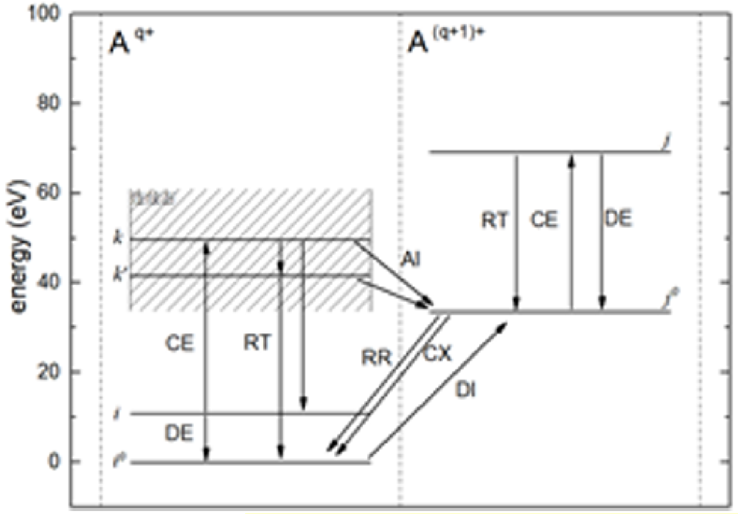

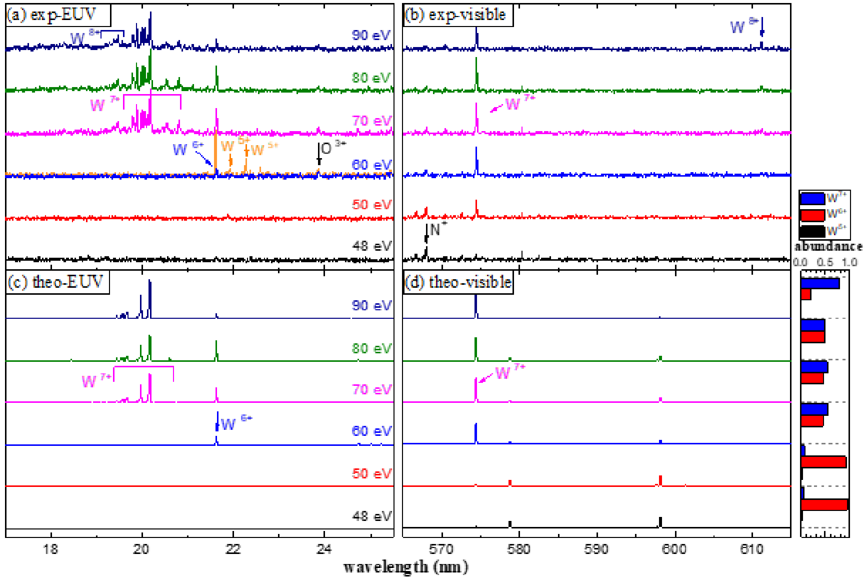

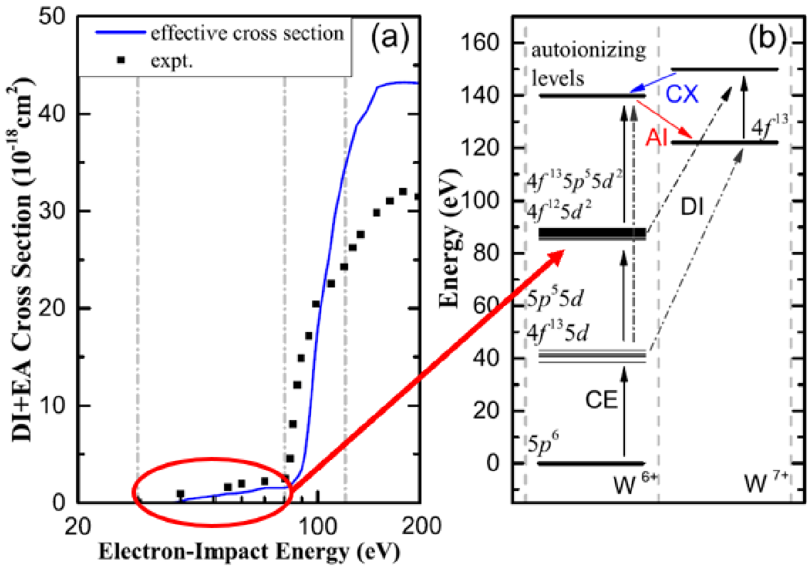

- Tungsten spectra were observed at the electron collision energy below the ionization potential of the corresponding tungsten ions.
- It is caused by metastable state ionization, in which bound electrons are excited during e-W collision. Once electrons are populated at metastable states, they can stay there for long time, e.g., a few ms.
- The excited ions could be ionized in the subsequential collisions. The two steps process, collisional-excitation and ionization, significantly reduced the ionization potential.

Q. Lu et. al, PRA, 99 (2019)
C.L. Yan et. al, PRA, 105 (2022)

Outline

- Tungsten and High-Z impurity source in EAST
- Impurity-related spectroscopic diagnostics in EAST
- Tungsten data needs and other important issues
- Relevant Activities
- Summary

Summary

ASIPP

- Tungsten behavior, transport study and its effective control is essential for the steady-state operation of Magnetic Confinement Fusion device.
- EAST has been operated with full W divertor, W guard limiter and Mo first wall since 2022 campaign.
- Sets of impurity-related spectroscopic diagnostics have been newly developed on EAST and became the powerful platform to study the impact of tungsten and other high-Z impurity behavior on plasma performance.
- Application of tungsten atomic data to quantitative analysis on tungsten spectra **is still very limited** compared to observation due to lack of reliable effective data. The main reason is the complexity and time-consuming of the modelling work.

- **It is very nice that IAEA is planning a Coordinated Research Project (CRP) on Tungsten Ions in Magnetic Confinement Fusion Plasmas.**
- **I would like to take this opportunity to work with international and domestic colleagues and make progress on this.**

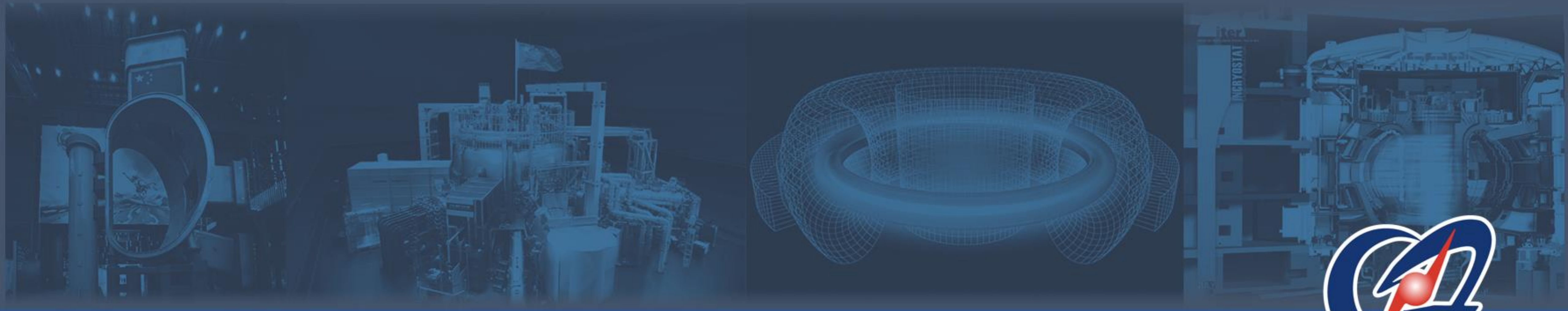

Thanks for your attention!

ASIPP

Dr. ZHANG Ling (张凌)
zhangling@ipp.ac.cn